



# Tectonics

## RESEARCH ARTICLE

10.1029/2019TC005825

### Key Points:

- The geological record of a major and extensive mid-Cretaceous tectonic phase in the Central Andes
- Inversion of Late Cretaceous extensional intra-arc basins due to a major tectonic phase on the western Gondwana margin
- Crustal response after a long-lived extensional period in an active subduction margin

### Supporting Information:

- Supporting Information S1

### Correspondence to:

D. Boyce,  
danielboyce@gmail.com

### Citation:

Boyce, D., Charrier, R., & Fariás, M. (2020). The first Andean compressive tectonic phase: Sedimentologic and structural analysis of mid-Cretaceous deposits in the Coastal Cordillera, Central Chile (32°50'S). *Tectonics*, 39, e2019TC005825. <https://doi.org/10.1029/2019TC005825>

Received 14 AUG 2019

Accepted 14 JAN 2020

Accepted article online 16 JAN 2020

## The First Andean Compressive Tectonic Phase: Sedimentologic and Structural Analysis of Mid-Cretaceous Deposits in the Coastal Cordillera, Central Chile (32°50'S)

Daniel Boyce<sup>1</sup> , Reynaldo Charrier<sup>1,2</sup>, and Marcelo Fariás<sup>1</sup>

<sup>1</sup>Departamento de Geología, FCFM, Universidad de Chile, Santiago, Chile, <sup>2</sup>Carrera de Geología, Universidad Andres Bello, Santiago, Chile

**Abstract** We document the effects of major mid-Cretaceous to Late Cretaceous compression within the volcanic arc of the western Gondwanan margin. The thinned Early Cretaceous Andean margin underwent rapid thickening and shortening-related exhumation of magmatic arc rocks during compressional inversion of late Early Cretaceous intra-arc basins. Clastic sedimentary and volcanic rocks recording this phase of initial Andean shortening correspond to the Las Chilcas Formation and are interpreted to have been deposited in a proximal retro-arc position. A detailed analysis of these deposits reveals multiple periods during sustained compressional deformation throughout the latest Early and Late Cretaceous, from 105 to 83 Ma. This deformation is evidenced by the exhumation of older units in the Coastal Cordillera, together with the development of contractional structures and a strong sedimentary response involving deposition of approximately 3 km of synorogenic nonmarine clastic deposits of the Las Chilcas Formation. The structures and associated deposits suggest that the strongest uplift and deformation period occurred from 100 to 95 Ma, whereas subsequent Late Cretaceous deformation was less pronounced, possibly a result of eastward migration of deformation. This tectonic phase coincided with similar coeval synorogenic deposits in Chile and other Andean regions, which have been attributed to initial Andean shortening resulting from a major plate reorganization.

### 1. Introduction

The transition between Early and Late Cretaceous represents a crucial moment in the evolution of the Andean mountain range, reflected by a shift from a predominant extensional period to compressional tectonic conditions that caused major tectonic and paleogeographic changes on the continental margin. This episode, originally named Peruvian tectonic phase (Mégard, 1984; Scheuber et al., 1994; Steinmann et al., 1929), has been interpreted as a result of a major geodynamic reorganization on Earth. In the western Gondwanan margin this phase is correlated with the plate reorganization that caused the northeastward displacement of the Farallon Plate with a positive trench-normal absolute velocity in the margin and a dextral oblique convergence between the oceanic and the South American plates (Horton, 2018a; Larson & Pitman, 1972; Maloney et al., 2013 and Somoza & Zaffarana, 2008). The tectonic conditions developed at this moment initiate a new stage of Andean evolution characterized by dominant compression and mountain building and therefore, this episode can be considered as the first orogenic phase in the development of the Andes.

The compressive tectonic conditions caused an abrupt paleogeographic modification characterized by (i) a generalized uplift of the continental margin, generating relief and exhumation of the magmatic arc, (ii) the development of a continental basin to the east of the arc and the retreat of the sea as a product of the deformation of the Jurassic and Early Cretaceous marine back-arc deposits, and (iii) a rather wide, mostly continental forearc region to the west of the arc (Bascañán et al., 2016; Cecioni, 1957; Charrier & Vicente, 1972; Di Giulio et al., 2017; Horton et al., 2016; Horton & Fuentes, 2016; Mpodozis & Ramos, 1990 among others).

Despite the importance of this phase, little has been made in central Chile to thoroughly analyze the sedimentology, the chronology and to characterize the structural features affecting the associated deposits. The latter are grouped in the Las Chilcas Formation, exposed along the eastern slope of the Coastal Cordillera, between 32°S and 34°S (Figure 1).

The scarce geochronological control for the Las Chilcas Formation and the reduced knowledge of its internal stratigraphic and structural complexity has hindered previous authors to constrain the distribution and age of the different members and establish regional correlations between them; this has prevented a robust tectonostratigraphic interpretation of the unit and its general tectonic significance. Similarly, since no synorogenic deposits have been described for this stage in central southern Chile (Charrier et al., 2007), the connection between the intensively studied petroleum-rich foreland basin (Neuquén and La Ramada basins), the Late Cretaceous arc, and its deposits remains unclear. These uncertainties have prevented a full understanding of the extent and effects of this major late Early Cretaceous paleogeographic reorganization in the arc and proximal areas in this region of the Andes.

We present detailed stratigraphic, sedimentologic, and provenance analyses of the Las Chilcas Formation deposits resulting from the major mid-Cretaceous Peruvian tectonic phase and the associated paleogeographic modifications to fully understand its significance and paleogeographic consequences. Based on the results obtained from these analyses and the present-day knowledge of the tectonic evolution in this region, we infer the tectonic mechanisms that could have originated the structures affecting the Las Chilcas Formation. Finally, we intend to correlate the studied deposits with other coeval deposits in Chile and neighbor regions and discuss the possible tectonic setting where the Las Chilcas basin was located.

## 2. Tectonic and Geologic Setting

The long and complex evolution of the western margin of South America in central Argentina and Chile shows a succession of varied tectonic settings. From the Late Triassic to earliest Jurassic, after a period of arrested continental rift and possibly low rate subduction conditions, a renewed subduction caused a major paleogeographic reorganization along western Gondwanan that lasted until the end of the Early Cretaceous (Charrier et al., 2007; Mpodozis & Ramos, 1990). During this cycle slab rollback caused extension on the margin and crustal thinning (Rossel et al., 2013). Subduction-related magmatism formed a well-developed volcanic arc along the present-day coastline characterized by thick primitive volcanic sequences and marine sediments intercalations (Oliveros et al., 2007; Vergara et al., 1995). The volcanic arc separated the oceanic realm, to the west, from an interior sea or back-arc basin, to the east (Charrier et al., 2007; Mpodozis & Ramos, 1990). In central Chile, the Jurassic and Early Cretaceous volcanics corresponding to this stage are exposed on the Coastal Cordillera (Figures 1 and 2), next to the Paleozoic intrusives, which mostly border the Pacific coast. The exhumation of the Paleozoic and Jurassic intrusive units took place between 106 and 91 Ma, based on apatite fission track dating of three samples in the Coastal Cordillera by Gana and Zentilli (2000) and Gana and Tosdal (1996).

The Early Cretaceous units conform an east dipping homocline comprised by the thick volcanic and marine Lo Prado Formation (~145 to ~132.9 Ma) and by the ~5,000 m thick primitive volcanic (flood-basalt-type lavas) Veta Negra Formation (~132.9 to ~117 Ma) (Aguirre et al., 1999; Fuentes et al., 2005; Rivano et al., 1993). Based on geochemical data and on their great thicknesses, Vergara et al. (1995) and Charrier et al. (2007, 2015) proposed that these Early Cretaceous formations were deposited in a strongly subsiding extensional tectonic basin; however, no solid structural evidence defining the type and architecture of the basin have been documented. On this basis, they have been considered as synrift sequences (Figure 2). The Veta Negra Formation is overlain by the 1.5 km thick volcanic and tuffaceous Cerro Morado Formation (Carter & Aliste, 1962). In the area of this study the Early Cretaceous formations are intruded by the Late Cretaceous and 60 km wide Caleu pluton. This intrusion is made of at least four dioritic to monzogranitic intrusive pulses with zircon  $^{208}\text{Pb}/^{235}\text{U}$  age ranges from 99.7 to 94.2 Ma (Molina, 2014; Parada et al., 2005). Based on  $\text{Ar}^{40}/\text{Ar}^{39}$  plateau ages in biotite, amphiboles, and plagioclase Parada et al. (2005) interpreted a rapid exhumation event for this pluton from 94.9 to 93.2 Ma and based on apatite fission track results a subsequent slower one at 94–90 Ma.

From late Early Cretaceous time new tectonic conditions and a new tectonic setting prevailed on the western margin of Gondwana (Charrier et al., 2007; Horton, 2018a; Horton, 2018b; Horton & Fuentes, 2016; Mpodozis & Ramos, 1990). This episode is evidenced by unconformities in the retro-arc deposits, rapid sediment accumulation, and changes on the retro-arc basins provenance (Bascuñán et al., 2016; Cecioni, 1957; Charrier & Vicente, 1972; Di Giulio et al., 2017; Horton et al., 2016; Horton & Fuentes, 2016; Keidel, 1925; Mégard, 1984; Mpodozis & Ramos, 1990; Steinmann et al., 1929; Windhausen, 1931, etc.).

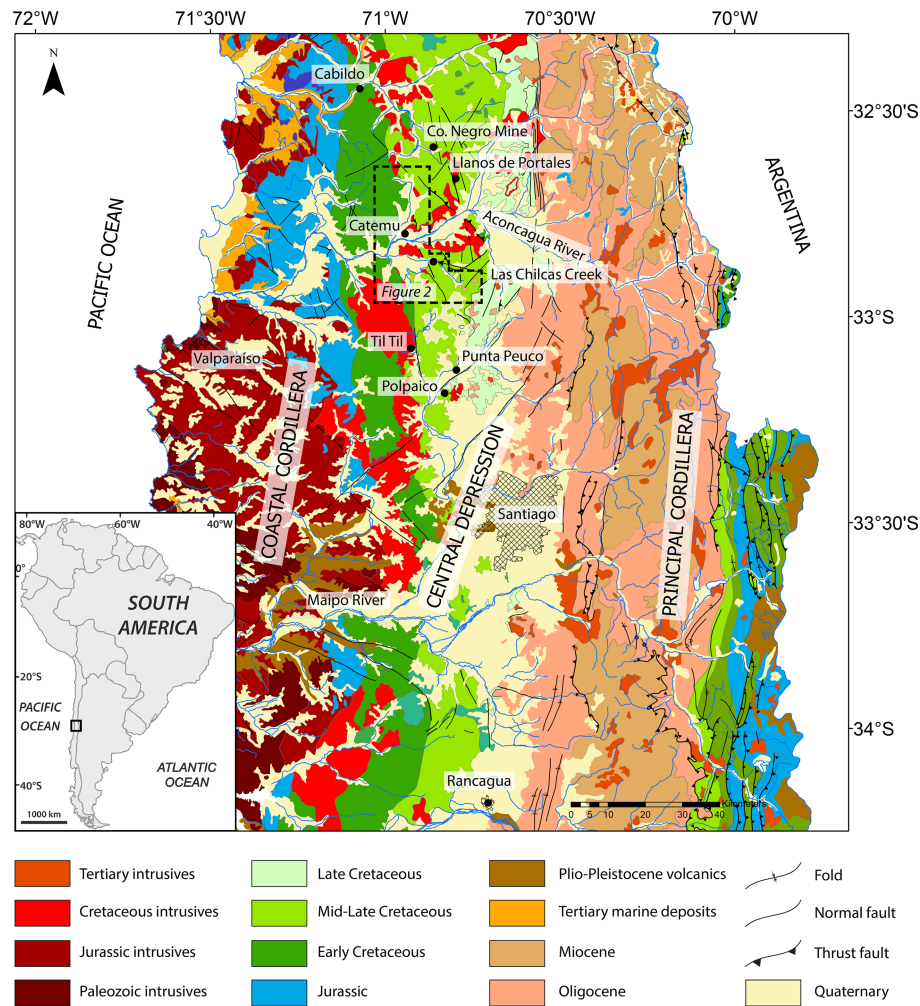


**Figure 1.** Simplified geological map of central Chile based on SERNAGEOMIN (2003) showing all the relevant localities for the study and the main regional geographic features. The dashed line polygon indicates the location of the area of study.

Along the eastern slope of the Coastal Cordillera the Las Chilcas Formation (Figure 3) (Boyce, 2015; Gana & Wall, 1997; Rivano et al., 1993) unveils clear facies change from the Early Cretaceous volcanics to Late Cretaceous coarse and high-energy sediments (Figure 2). This formation is interpreted to be contemporaneous to the described tectonic phase; however, it has been historically assigned to a wide age range, from Early to Late Cretaceous (Gallego, 1994; Godoy et al., 2006; Rivano et al., 1986, 1993; Thomas, 1958; Tunik & Álvarez, 2008; Wall et al., 1999). Due to the scarce geochronological control in it and the strong lateral and vertical facies variations, there has been no consensus about its subdivision in members and its age range.

Resting unconformably and flat-lying on the Las Chilcas Formation, the Late Cretaceous Lo Valle Formation (70–73 Ma) consists of up to 1,800 m of tuffs interbedded with andesitic breccias and conglomerates (Gana & Wall, 1997).

### 3. Stratigraphic and Sedimentologic Characterization of the Las Chilcas Formation

We describe next the stratigraphy for the Las Chilcas Formation, divided in four members documented from bottom to top in the area of study. The method how these sections have been constructed and the facies analysis method is detailed in Text S1 in the supporting information. Initially, Boyce (2015) named the

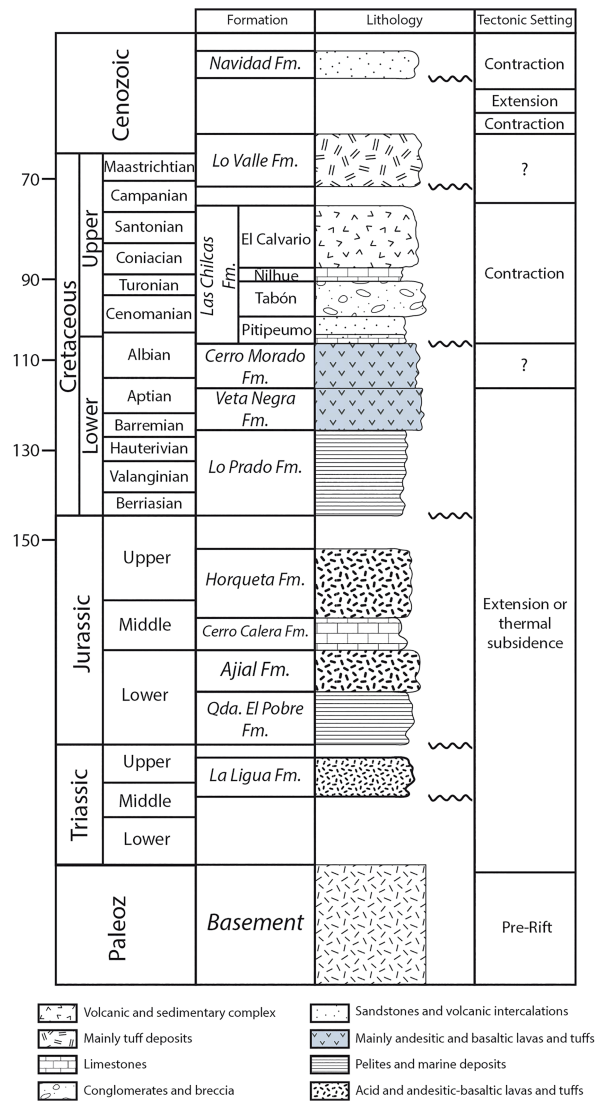


**Figure 2.** Generalized stratigraphic column of the Coastal Cordillera based on previous studies in the area (Carter & Aliste, 1962; Charrier et al., 2007; Rivano et al., 1993) and on this study.

stratigraphic units here documented with capital letters from A to U, including sections of the Veta Negra and Cerro Morado Formations, which are not subject of the present study. We have kept the same nomenclature but only to refer to those stratigraphic units in the Las Chilcas Formation corresponding to capital letters from D to U. The stratigraphic sections are displayed in Figure 4, and their geographic location can be found in Figure 3. The relevant facies mentioned in the text and displayed in the stratigraphic sections are described in Table 1.

### 3.1. Pitipeumo Member: Lagoon, Shallow Braided River, and Distal Alluvial Fan Systems

The Pitipeumo Member rests on angular unconformity on the Cerro Morado Formation (Figure 5a) representing the basal member of the Las Chilcas Formation (Arévalo, 1992; Espinoza, 1969; Viteri, 1970) (Figure 3). South of the Aconcagua Valley, directly overlying the volcanic Cerro Morado Formation strongly weathered fine grained calcareous sandstones were documented with a preserved thickness of about 30 m (within Unit D). Similarly, marine stromatolitic algal, as well as fan delta and lagoon lithofacies have been documented at the base of the Las Chilcas Formation by Arévalo (1992) and to the south

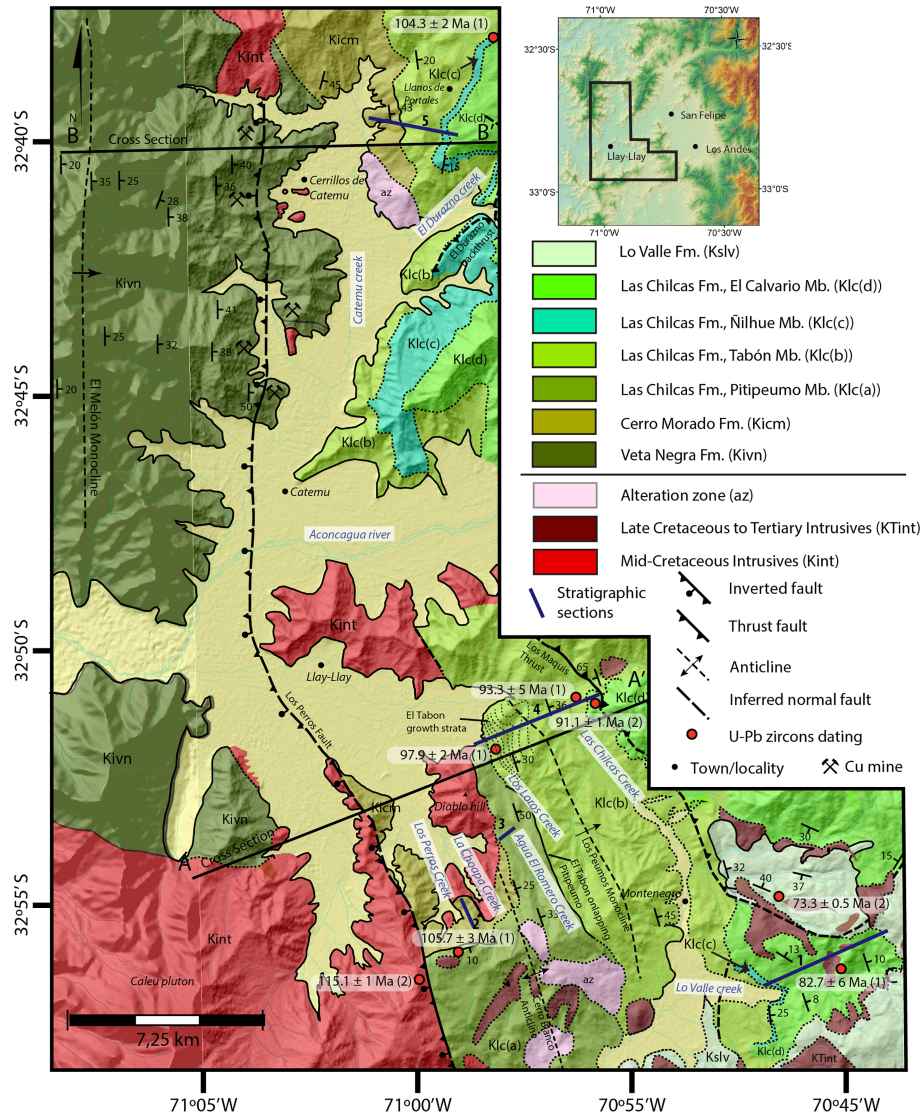


**Figure 3.** Geological map of the study area including ages obtained in this study. (1) Mean weighted U-Pb ages for igneous zircons; (2) Youngest detrital U-Pb zircon age.

of the area of this study at the locality of Polpaico (see location in Figure 1) by Gallego (1994) and Corvalán and Vergara (1980).

The basal marine calcareous horizon underlies a 150 m sequence of sandstones, conglomeratic sandstones, and conglomerates (Unit E). In some localities no calcareous beds exist, and the conglomerates of Unit E rest directly on the Cerro Morado Formation (Figure 5a). Three lithofacies represent the main depositional processes in this portion of the Pitipeumo Member: poorly sorted, clast-supported conglomerate (Gth), matrix-supported conglomerates (Gmm), and massive sandstones (Sm), whereas thin beds of massive siltstone (Fm), though present, are rare. The dominant depositional process of this conglomeratic sequence is interpreted as traction currents in erosive flows. From the lithofacies analysis we interpreted that the conglomerate beds of this unit represent a shallow braided gravel bed system (according to Miall, 1996).

Representing the top of the Pitipeumo Member in this section and covering the basal conglomerates is a 90 m thick dacitic-andesitic lava succession (Unit F), which in turn is covered by, at least, 10 m of conglomerates and sandstones. The thick volcanic intercalation toward the top of the member records the active volcanism in the area.

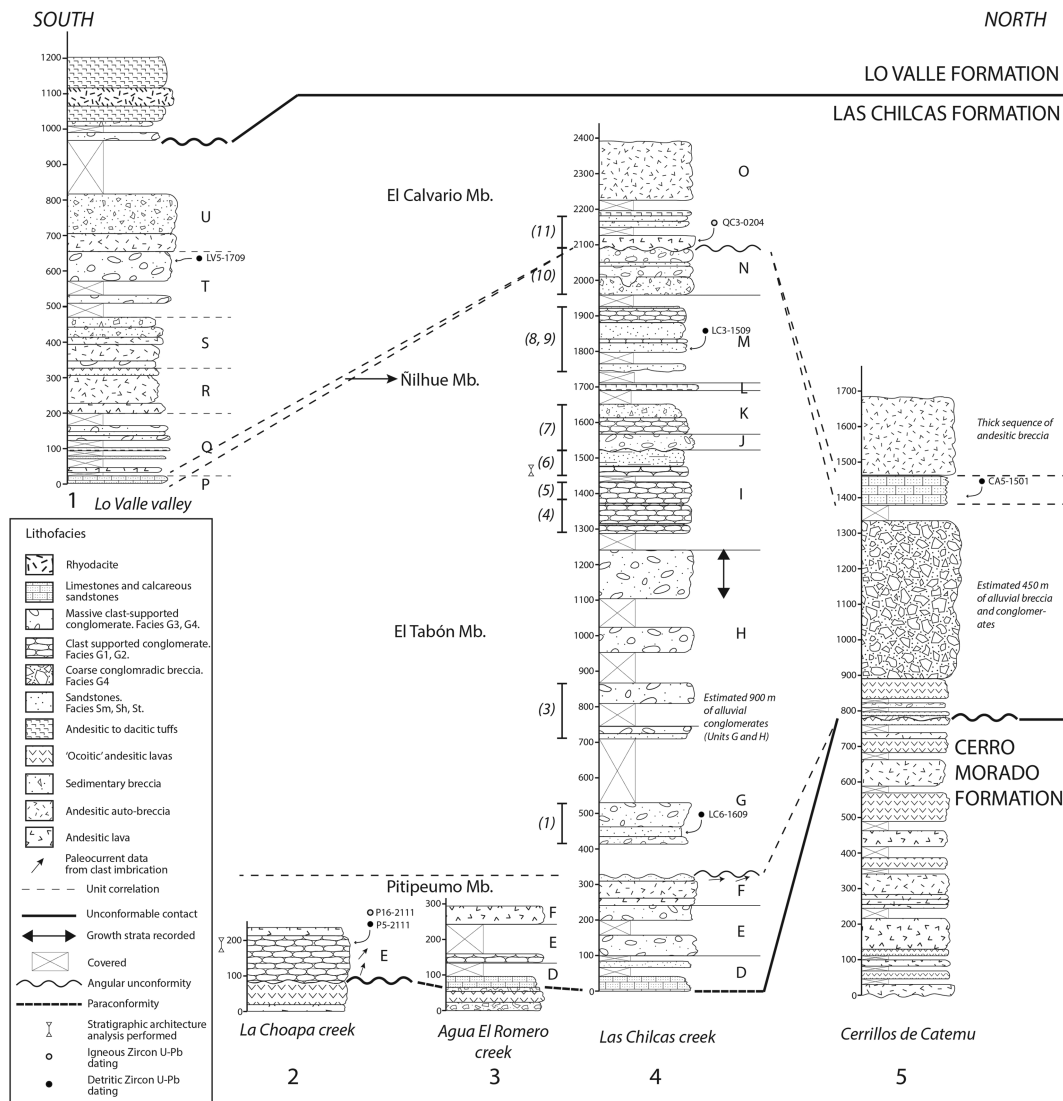


**Figure 4.** Measured stratigraphic sections from north and south of the Aconcagua Valley. The diagram includes lithologies, lithofacies, stratigraphic correlations, paleocurrent data, and locations of U-Pb zircon age datings.

### 3.2. Tabón Member: Alluvial Fan System and Shallow Braided and Wandering Fluvial Systems

North of the Aconcagua Valley, in the Cerrillos de Catemu area (see location in Figure 3), the Tabón Member rests on angular unconformity on the Cerro Morado Formation (Figure 5b). Here, the base of the Tabón Member is clearly defined by the conglomeratic levels intercalated with few andesitic flows for about 100 m, and on top of this rests a 500 m thick homogeneous sequence of matrix-supported coarse conglomerates and sedimentary breccias (Gmm). Thus, somehow different to what is described next south of the Aconcagua Valley, the Tabón Member here is dominated by Gmm facies, with almost no fine-grained intercalations, indicating the continuous discharge of debris flows in a proximal alluvial fan environment.

South of the Aconcagua Valley, at the Las Chilcas Creek, the 1,750 m thick conglomeratic Tabón Member unconformably onlaps the Pitipeumo Member and can be subdivided in nine successive units named from G to N (Figure 4) each of them with its own prevailing sedimentary system. Here, the lower deposits of the Tabón Member fill a deep incision in the Pitipeumo Member, which evidences an important erosion process before the deposition of the Tabón Member (further discussed in section 5.1).

At the bottom, Unit G fills in the described incision; massive matrix supported pebble-boulder conglomerates (Gmm) interbedded with massive pebbly sandstones (Sm), occasional intercalations of poorly sorted

**Table 1**  
*Facies Classification*

Facies in this study	Miall's facies	Description	Interpretation
Gcm	Gcm, Gp	Structureless massive clast-supported conglomerate, well sorted and rounded, with erosive bases.	Channel filling in declining stages and bar accretion.
Gth	Gcm, Gt, Gp, Gh	Regularly sorted pebble to cobble clast-supported conglomerate. Shows imbrication, horizontal bedding, and though cross bedding.	Longitudinal and frontal bars; channel filling.
Gmc	Gmc	Structureless massive pebble to boulder conglomerate, poorly sorted and rounded, clast supported. Nonerosive bases.	Hiperconcentrated flows.
Gmm	Gmm	Structureless massive pebble to boulder conglomerate, matrix supported, and poor to regular selection.	Debris flows
Bm	Gmm	Massive breccia, regular to poor selection. Clast size from pebble to cobble, matrix-supported, crystal rich.	Hiperconcentrated flows, associated to lahar
Sm	Sm	Fine to coarse massive sandstone.	Sediment gravity flows
Sh	Sh	Fine to coarse horizontally laminated sandstone; presents some pebbly levels.	Critic flow
St	St	Fine to coarse sandstone, pebbly in some places. Tough cross bedding.	Dunes (lower flow regime)
Fm	Fm	Massive mud and silt layers, present erosive bases and top.	Overbank, abandoned channel, or waning flood deposits.

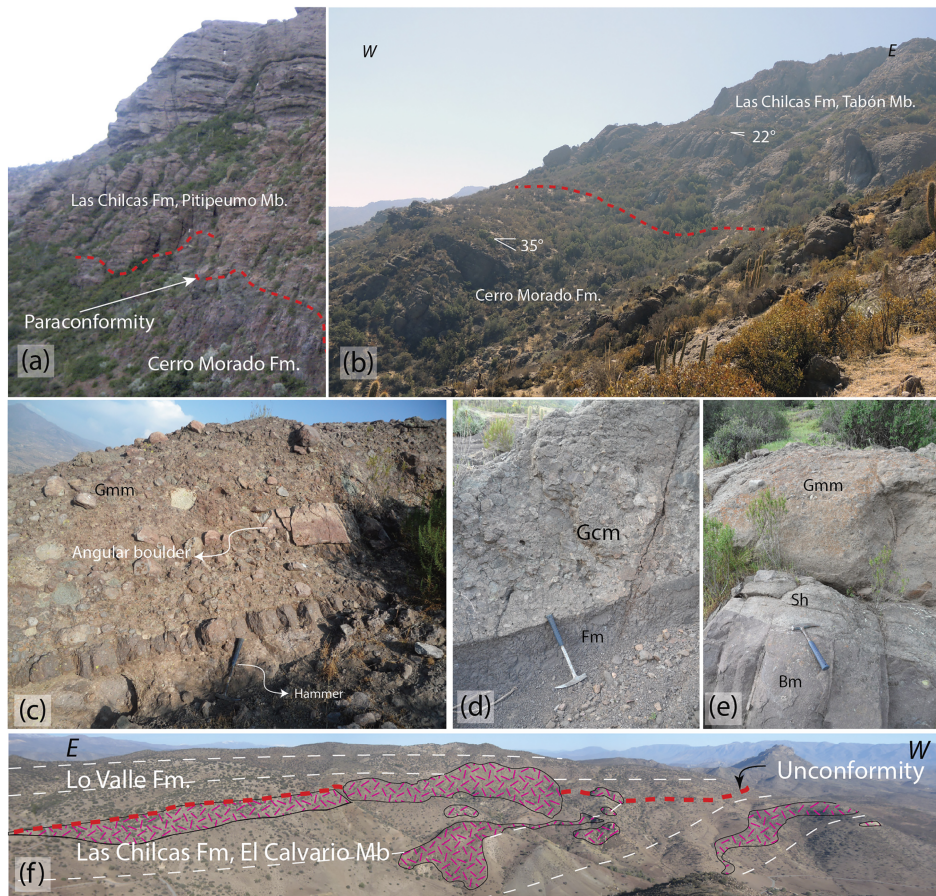


**Figure 5.** Photographs of the contact relationships of the Las Chilcas Formation in the study area and some of the characteristic facies of the Tabón Member. (a) Unconformity between the Cerro Morado Formation and Pitipeumo Member. (b) Unconformity between the Cerro Morado Formation and the Tabón Member in the Catemu Valley. (c) Massive poorly sorted Gmm facies in the Unit H of the Tabón Member. (d) Erosive contact between massive mudstone (Fm) and well-sorted gravel (Gcm) in Unit I in the Tabón Member. (e) Bm-Sh-Gmm lithofacies association in Unit L in the Tabón Member. (f) Angular unconformity (red line) between the El Calvario Member of the Las Chilcas Formation and the Lo Valle Formation; intrusives bodies are shown with a red pattern.

clast-supported conglomerates, and a few thin beds of massive siltstone (Fm), totalize a thickness of ~300 m (Unit G). The lithofacies assemblage in this unit is characteristic of alluvial fan depositional systems (Blair & McPherson, 1994; DeCelles et al., 1991; Miall, 1996).

Still filling in the upper part of the incision, an ~500 m thick homogeneous and massive conglomerates sequence (Unit H) conformably covers Unit G. This sequence is made of facies Gmc and Gmm, with some blocks of decametric size (Figure 5c). Several amalgamated conglomerate layers of these facies form massive vertical outcrops of up to 15 m of thickness. The interpretation of this unit is in many ways identical to that of Unit G; nevertheless, the lack of massive pebbly sandstones (Sm) beds indicates a continuous ingress of high-energy debris and pseudoplastic flows, a distinctive characteristic of proximal or young alluvial fan systems (Blair & McPherson, 1994).

Conformably overlying Unit H is Unit I (~225 m), which conglomerates (Gcm and Gth) intercalated with massive siltstone (Fm) make up its main lithofacies association (Figure 5d), indicating traction transport in turbulent flows. The lack of sandstone lenses or beds, and gradation trends in the conglomerates suggests a steady high-energy discharge. Similar deposits with strong variations in the flow direction and lacking important sandstone lenses were interpreted by Miall (1996) as the product of gravel bed wandering rivers.

Above Unit I, the ~55 m thick Unit J is made of conglomerates (Gmm) intercalated with both massive (Sm) and horizontally bedded sandstones (Sh) with thicknesses of 30–50 cm. As previously discussed, such successions are typically interpreted as the product of a proximal alluvial fan systems.

The overlying Unit K (~70 m) consist of a homogeneous succession of 0.5 cm to 1.5 m thick conglomeratic beds (Gth) interbedded with horizontally bedded 20–30 cm thick sandstone layers (Sm, Sh) with erosive bases. As discussed for the Pitipeumo Member, the interpretation of the Gth-Sh-Sm lithofacies association represents deposits of a shallow gravel bed braided river.

Conformably over Unit K, a reddish and strongly oxidized tuffaceous layer (~30 m) comprises Unit L. To the east of the Las Chilcas Creek and overlying Unit L, the units M and N (~350 m) consist of gray massive sandstones (Sm), massive conglomerates (Gmm), crystal-rich breccias (Bm), and some massive siltstones (Fm) (Figure 5e), which association would represent mainly distal and proximal alluvial fan system and a wandering fluvial system. A major incision in the base of Unit N is infilled with a massive, matrix-supported conglomerate (Gmm), which is included in the same unit.

### 3.3. Ñilhue Member: Limestones

North of Aconcagua Valley, Carter and Aliste (1962) defined a calcareous unit resting on the Tabón Member as the Ñilhue Member. This consists of thin-bedded limestone layers containing fossils of mollusks, fresh water clams, plant remains, and wood fragments, indicating a fresh water origin (Carter & Aliste, 1962; Elgueta et al., 1990; Sánchez, 1968). At the type locality, the reported thickness of the Ñilhue Member is ~825 m (Carter & Aliste, 1962); however, given the considerably smaller thickness observed in other regions during this study and the structural complexity observed in the Ñilhue area, this thickness is possibly exaggerated due to structural repetitions.

South of the Aconcagua Valley, at the Las Chilcas Creek (Figure 3), this Member is not preserved and hence the upper El Calvario Member rests directly on the Tabón Member. Yet, 14 km to the SW of the Las Chilcas Creek, a 25 m thick limestone layer (Unit P) is exposed. This calcareous unit, presenting chert nodules, and some marl and calcarenitic intercalations, is strongly weathered and locally marbled by the effect of an Oligocene dioritic intrusion. Godoy (1982) described in this member algae fossils indicating a lagoon environment, a conclusion that differs from the continental origin assigned by other authors and causes uncertainties about its depositional environment. Nonetheless, we interpret from the stratigraphic position that these limestone beds (Unit P) correlate to the Ñilhue Member.

### 3.4. El Calvario Member: Renewal of the Volcanic activity

On top of the Ñilhue Member, the El Calvario Member was originally defined as the base of the Lo Valle Formation (Carter & Aliste, 1962). Nevertheless, based on its stratigraphic position, lithological similarity, and the new ages presented in section 4, we have included this as the upper member of the Las Chilcas Formation. At the Las Chilcas Creek, the El Calvario Member unconformably overlies the Tabón Member



in absence of the Ñilhue Member. The El Calvario Member in this locality seals the deformation that affects the Tabón Member with a back thrust fault (Los Maquis thrust, further described in section 5.1).

In the stratigraphic section completed at the Lo Valle creek, the El Calvario Member was subdivided into five conformable units (Q to U) (Figure 4), which are unconformably covered by the Lo Valle Formation (Figure 5f). Unit Q (~150 m) is characterized by matrix-supported conglomerates (Gmm) with a fine-grained and intensely hematitized matrix. Above, Unit R (~130 m) rests on Unit Q and consists of andesitic lavas and breccia. The overlying Unit S (~180 m) is also mostly made up of andesitic lavas, but it includes three conglomeratic intercalations of clast-supported and poorly selected (Gmc) clasts. Unit T (~180 m) is characterized by massive, clast- and matrix-supported conglomerates (Gmc and Gmm). Finally, Unit U commences with a 50 m thick succession of andesitic lavas that grade upward to 130 m of conglomerates (Gmm) and sedimentary breccias. From the matrix-supported array and the variable grain size of all sedimentary units in the El Calvario Member, the main depositional processes that took place between the volcanic events can be interpreted as debris flows of different energies. The significance of the volcanic units in this member indicates the renewal of an intense volcanic activity in the Las Chilcas basin.

### 3.5. Summary of the Sedimentary Environments

The presented stratigraphic and sedimentological characterization allows to understand the distribution of the units and members in the study area (Figure 3) and the paleogeographic changes that took place during the deposition of the Las Chilcas Formation. The main documented environments are (1) marine ingression recorded by the basal limestone layers during the initial stages of the Pitipeumo Member; (2) shallow gravel bed wandering river systems in some stages of the Pitipeumo and Tabón members; (3) alluvial fan system during most of the Tabón and the El Calvario members; (4) continental or marine water inundations recorded by the Ñilhue Member; and (4) intense volcanic activity in parts of the Pitipeumo and El Calvario members.

## 4. U-Pb Geochronological Results

### 4.1. Sampled Levels

To constrain the age of the Las Chilcas Formation and to determine which units were under erosion during its deposition, five U-Pb age determinations on detrital zircons have been carried out south of the Aconcagua Valley and one north of the valley (Figures 3 and 6). With the same objective, one U-Pb dating was carried out on igneous zircons of a tuff clast collected from the base of the Las Chilcas Formation. In order to constrain the depositional age, two U-Pb zircon datings were made on volcanic samples located at the top and bottom of the Las Chilcas Formation (Figures 3 and 6). Also, one igneous zircon U-Pb dating was done from a volcanic sample taken at bottom of the Lo Valle Formation. Finally, one sample from the Caleu pluton was dated by the same technique. A summary of all these radiometric datings performed in this study is exposed in Table 2. Likewise, the ages distribution can be observed in Figure 3. The depositional age basis, the dating method, the zircons textures, and the analytical data are detailed in Text S1 in the supporting information.

### 4.2. Igneous Zircon Ages

A crystal tuff clast sample (P16-2111) 150 m above the base of the Las Chilcas Formation yielded a mean weighted age of  $112 \pm 1.3$  Ma (Figure 6). Its age indicates that the clast likely derives from the underlying volcanic Cerro Morado Formation.

A mean weighted U-Pb zircon age of  $103 \pm 0.68$  Ma was obtained from 29 igneous zircons from a gray pyroxene andesite (PP3-1601) (Figure 6) exposed in the southern part of the study region, next to the locality of Punta Peuco (see locality in Figure 1). This volcanic succession overlies the Polpaico limestones, which we correlated with calcareous beds at the base of the Pitipeumo Member.

A mean weighted zircon age of  $91.1 \pm 0.74$  Ma from 31 zircons was obtained from a sample (QC3-0204) collected from a thick andesitic layer at the base of the El Calvario Member (Figure 6).

In the Lo Valle Creek, at the base of the Lo Valle Formation, a crystal tuff (ET31-1407) yielded a mean weighted age of  $73.3 \pm 0.45$  Ma from 31 zircons (Figure 6).

At the eastern boundary of the Caleu Pluton, close to the contact with the Las Chilcas Formation (see location in Figure 3), a strongly weathered phaneritic granodiorite sample (P3-2211) yielded zircon ages ranging

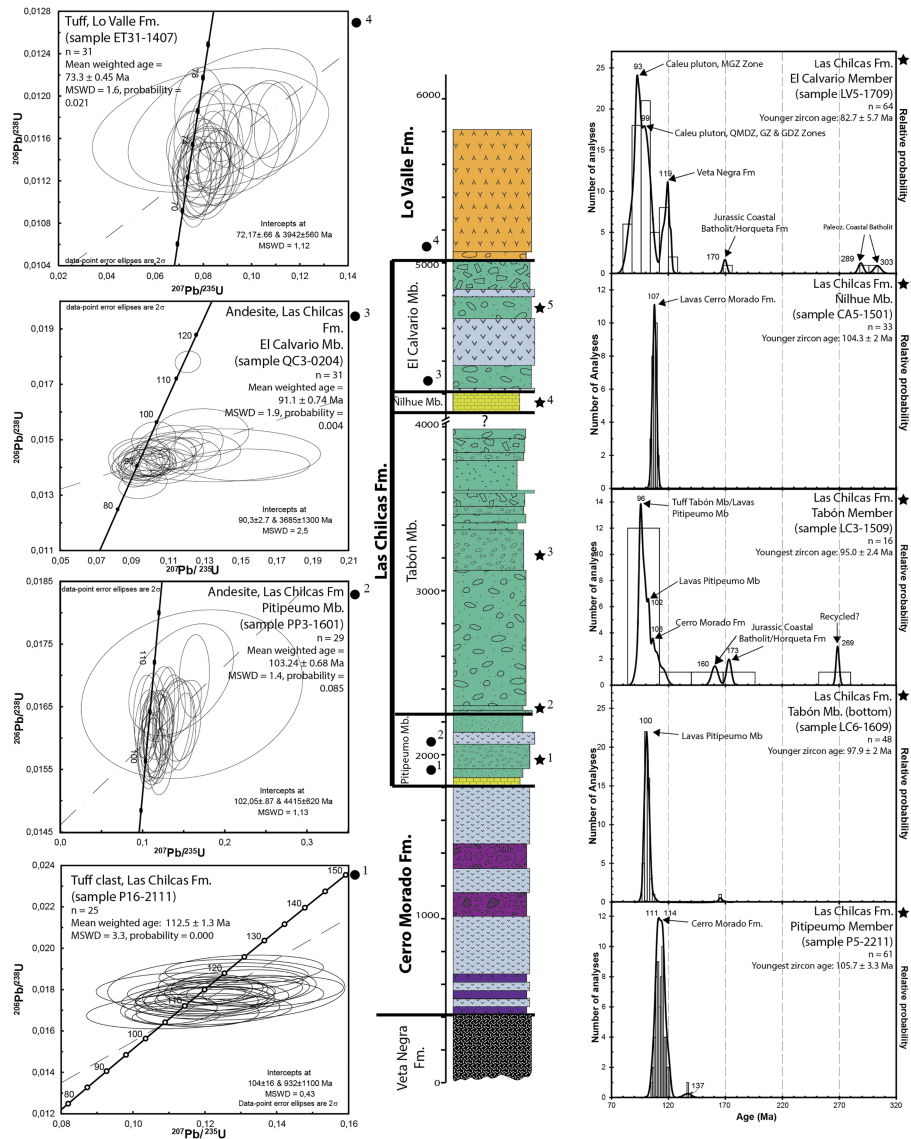


**Figure 6.** In the middle a generalized section of the Las Chilcas Formation and the adjacent formations. In the left side U-Pb Concordia for the igneous samples analyzed in this study and the respective stratigraphic location of the sample marked in the section with a bold circle and a number. In the right side, U-Pb probability plots from the detrital samples analyzed in this study and the respective stratigraphic location of the sample marked in the section with black star and a number.

from  $109.0 \pm 3.8$  to  $123.4 \pm 1.9$  Ma, with a mean weighted age of  $115 \pm 1$  Ma (see Concordia in the supporting information). This age is much older than the ages previously obtained from this pluton (89 and 106 Ma) (Molina, 2014), thus suggesting the existence of older magmatic pulses in the eastern edge of the pluton.

### 4.3. Detrital Zircons Ages

**Pitipecumo Member:** A sandstone sample (P5-2211) provided 100 zircon grains that yielded ages between 105 and 121 Ma (Figure 6); it was taken in the same layer where the crystal-tuff clast (sample P16-2111) was collected, 150 m above the basal contact with the Cerro Morado Formation. Zircons from this sample form a single peak with a flat top and ages ranging between 111 and 114 Ma. The youngest zircon age with a discordancy <10% is  $105.7 \pm 3.3$  Ma representing the depositional age.

**Tabón Member:** in the base of the Tabón Member 104 zircons grains from a fine arkose layer were analyzed (LC6-1609) (Figure 6). All the analyzed zircons yielded a single peak at 100 Ma, which can be interpreted as

**Table 2**  
*Age Dating Samples Summary*

Sample ID	X_UTM_WGS84	Y_UTM_WGS85	Rock type	Mineralogy/clasts by importance	Texture	Mean weighted age	Max deposition age	Youngest Zircon age
LC3-1509	326642	6363515	Medium arkose	Felspar, volcanics, clays	Clastic		96 Ma	95.0 ± 2.4 Ma
LV5-1709	336200	6353816	Quartzwake	Qtz, Kspar, Mgt	Clastic		93 Ma	82.7 ± 5.7 Ma
P16-2111	322766	6354590	Crystal tuff	Qtz, Kspar, volcanics	Piroclastic	112.5 ± 1.3 Ma		
P5-2211	322851	6354612	Medium sandstone	Qtz, Plg, volcanics	Clastic		111 Ma	105.7 ± 3.3 Ma
P3-2211	321008	6353935	Granite	Qtz, Plg, Kspar, Amph	Phaneritic	115.1 ± 1 Ma		
QC3-0204	326751	6364076	Amphibole trachyte	Plg, Kspar, Amph, Qtz	Seriate	91.1 ± 0.74 Ma		
ET31-1407	333623	6356646	Crystal tuff	Plg, Qtz	Piroclastic	73.3 ± 0.45		
LC6-1609	323513	6361909	Medium arkose	Qtz, Felspar, volcanics	Clastic		100 Ma	97.9 ± 2 Ma
CA5-1501	325114	6389417	Calcareous sandstone	Cct, Qtz	Carbonatic		107 Ma	104.3 ± 1.6 Ma
PP3-1601	329639	6336462	Piroxene andesite	Kspar, Plg, Px, Mgt	Porphyritic	103.24 ± 0.68 Ma		

the maximum depositional age. The age of the youngest zircon with a discordancy <10% is  $97.9 \pm 2$  Ma, representing the depositional age. Given the small number of zircons with discordance <10% in this sample and in order to have a more complete record, we have considered all the zircon ages with discordance values <20% ( $n = 48$ ) for the provenance analysis.

Toward the middle to upper portion of the Tabón Member, 27 zircons were obtained from a medium grained sandstone (LC3-1509) (Figure 6). Due to the small number of zircons the obtained age is statistically weak. Taking into consideration the most important and youngest probability peak, the maximum depositional age is 96 Ma. The youngest zircon age with a discordancy <10% is  $95.0 \pm 2.4$  Ma, which is likely the depositional age. For the provenance analysis zircons with discordance <15% ( $n = 16$ ) were considered.

Ñilhue Member: The single dated sample in this member was collected north of the Aconcagua Valley (CA5-1501) in a strongly weathered limestone layer. In this sample, 100 zircons crystals were analyzed (Figure 6). The probability plot shows a single peak at 107 Ma. The Concordia diagram shows a lower intercept at  $99.5 \pm 8.3$  Ma. The youngest zircon age with a discordancy <10% yielded  $104.3 \pm 1.6$  Ma. Because the results show highly discordant values, and in order to obtain enough data for the provenance study, zircons grains with discordances <20% ( $n = 33$ ) were considered for this specific objective.

El Calvario Member: Toward the top of the Las Chilcas Formation, in the Lo Valle Creek (see location in Figure 3), a fine arkosic quartz-wake was sampled (LV5-1709) and 100 zircons extracted to be analyzed (Figure 6). The maximum depositional age is recorded by the most important and youngest probability peak at 93 Ma. The rest of the zircon ages form a cluster between  $84.2 \pm 6.5$  and 100 Ma. The age of the deposit would be that of the youngest zircon, which is  $82.7 \pm 5.7$  Ma, with a discordancy of 0.36%; however, given the wide error associated with this result, it is difficult to assign a precise deposition age. In turn, considering the U-Pb zircon age of  $91.1 \pm 0.74$  Ma from the QC3-0204 lava, collected near the top of this member, the age of this layer is likely close to the maximum age within error of the youngest zircon age, hence, about 88 Ma. For the provenance analysis, only zircons with a discordance <10% ( $n = 64$ ) were considered.

## 5. Structures and Structural Style

As has been described, the Las Chilcas Formation evidences major lateral and horizontal stratigraphic variations. This suggests the existence of an intense tectonic activity coeval with its deposition. In order to

understand what structures may have influenced this process, we describe those most relevant observed in the area.

### 5.1. South of the Aconcagua Valley

South of Aconcagua Valley is the east vergent asymmetrical Cerro Blanco anticline (Figure 7a), which core is made of the Cerro Morado Formation and the Pitipeumo Member. This structure extends with a NNW-SSE striking hinge line for over 12 km (see Figure 3) and presents an almost flat back limb and a steep frontal limb, features suggesting a thrust propagation fold origin (Suppe & Medwedeff, 1989). The lower part of the frontal limb consists of 50° east dipping layers of the Pitipeumo Member, which are unconformably overlapped by the 30° east dipping conglomerates of the Tabón Member (Figures 7b and 7c; onlap location labeled in Figure 3). At the Los Loros Creek (see location in Figure 3) this onlap occurs with a slightly different architecture: The 30° east dipping Tabón Member layers fill up a deep incision generated in the 50° east dipping Pitipeumo Member volcanics (Figure 7b), evidencing a strong erosion process that took place before or during the Tabón Member deposition. This intraformational unconformity (between the two members) constrains the initial development of the anticline prior to deposition of the Tabón Member. East of the onlap, on the eastern limb of the anticline, the Tabón conglomerates show an upsection decrease in dip and a lateral, eastward thickening of the beds conforming a growth strata geometry (Figure 7d) (see growth strata location labeled in map of Figure 3). This feature was generated during the development of the Cerro Blanco anticline while the Tabón Member was deposited. The growth of the anticline under compressive stress is supported by the record of 13 slickensides measured on the frontal limb showing reverse movement and by minor inverse faults recorded in the conglomerate layers of the Tabón Member also on the frontal limb.

West of the Cerro Blanco anticline crops out the Caleu Pluton (Figure 3). A steep west dipping fault (Los Perros Fault) is exposed on the contact between this unit and the Las Chilcas Formation (Figures 7e and 7f). Scarce slickensides and shear fractures preserved in the fault zone (Figure 7f) suggest thrusting of the Caleu pluton over the Las Chilcas Formation. Locally, zones with intense argillic alteration are affected by inverse faults that form east vergent duplexes. Despite the scarce structural information available on the fault to better understand its kinematics, the fact that the Los Perros Fault puts in contact the eastern and oldest units of the Caleu Pluton (113 Ma), which according to Parada et al. (2005) was emplaced at 7 km depth, with the much younger base of the Las Chilcas Formation (105 Ma), supports an east vergent reverse movement of this structure.

Three kilometers east of the Cerro Blanco anticline, the short wavelength Los Peumos monocline deforms the middle to upper section of the Tabón Member (location in Figure 3). This structure presents the same strike as the Cerro Blanco anticline, but its interlimb angle is more open. The eastern limb of the Los Peumos monocline is offset by a high angle, east dipping fault, the Los Maquis backthrust (Figure 7g). This fault thrusts the lower section of the Tabón Member over its upper section and is sub-horizontally sealed by the El Calvario Member, although a small amount of displacement can be observed in the lower El Calvario Member above the Los Maquis backthrust.

Finally, recording the youngest deformation occurred in the Las Chilcas Formation, in the Lo Valle creek (see location in Figure 3), the El Calvario Member exhibits an open hinge monocline with the frontal limb dipping 25° to the east, gently flattening eastward (Figure 5f). The Lo Valle Formation subhorizontally overlies this structure in an angular unconformity.

### 5.2. North of the Aconcagua Valley

North of the Aconcagua Valley, the absence of the Caleu Pluton allows observation of the structural features and the stratigraphic relationships between the Cerro Morado and the underlying Veta Negra and Lo Prado formations. These units form a massive N-S oriented and east dipping monocline—Melón monocline—that extends along its axis for over 40 km (see fold in map of Figure 3 and photo in the supporting information section). In its western side, the strata dip 20–30° to the east; The dip increases to the east reaching values of 50° at the Catemu Creek valley (Figure 3). In the central part of the monocline several N-S striking, subvertical normal faults were recognized. Along this valley a NS lineament with several occurrences of intrusions and hydrothermal alteration, which are presently mined for copper, suggests the presence of a deep-seated N-S structure (see Cu mining occurrences in Figure 3). We interpret that this lineament can

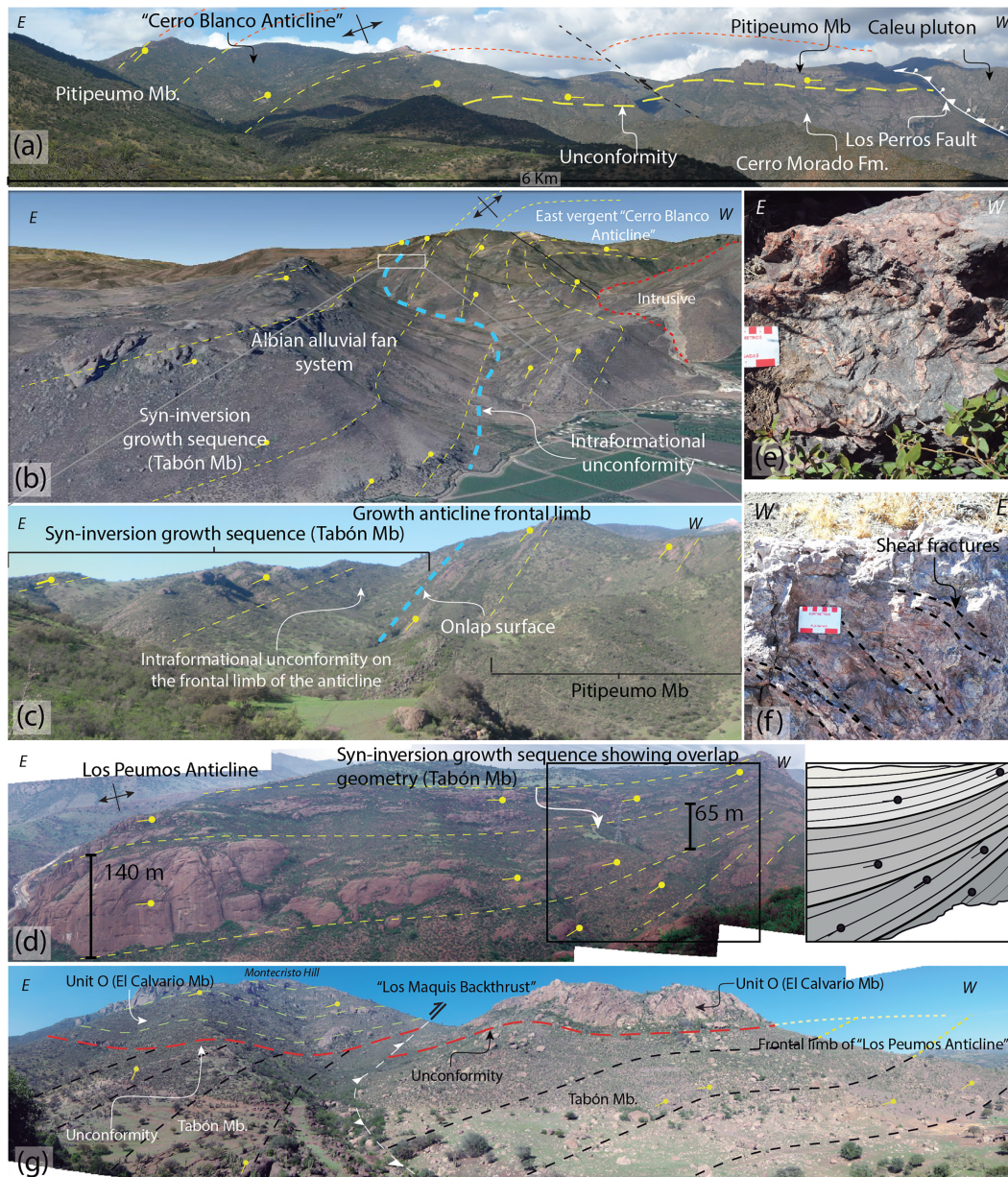


**Figure 7.** Relevant structures south of the Aconcagua Valley. (a) The asymmetrical Cerro Blanco Anticline in the Cerro Blanco Hill area. To the west, the Caleu Pluton overrides both the Cerro Morado and Las Chilcas formations. (b) Google Earth imagery showing the architecture of the frontal limb of the Cerro Blanco Anticline. Note the deep incision filled with alluvial deposits corresponding to the Tabón Member. (c) On the frontal limb of the Cerro Blanco anticline at the base of the growth succession of the Tabón Member anticline, detail of the onlap architecture. (d) On the frontal limb of the Cerro Blanco Anticline, the alluvial fan deposits of the Unit H of the Tabón Member show growth strata geometry. (e) Silicified rock in the Los Perros Fault zone. (f) East dipping shear fractures filled by clays in the Los Perros Fault zone. (g) The Los Maquis Backthrust, where lower levels of the Tabón Member override upper levels of the same member; above them, horizontally the lavas of the El Calvario Member.

be regarded as an extension of the Los Perros fault to the north; its geometrical implications are further discussed in section 6.4. East of this lineament the top of the Veta Negra Formation and the Cerro Morado Formation dip about 35° to the east and farther east are unconformably covered by the Tabón Member of the Las Chilcas Formation, dipping 20° to the east (see unconformity in Figure 5b). The presence of the Melón Monocline allows to estimate the potential thickness of the Veta Negra Formation of around 6,000 m in its thicker section—to the west of the Los Perros Fault—and about 3,500–4,000 m to the east of this structure (more details in section 6.4).

## 6. Discussion

### 6.1. New Chronostratigraphy and Sediment Provenance of the Las Chilcas Formation

According to the stratigraphic successions described, the ages obtained by previous authors and the new ages presented in this work (Table 2), it is possible to reconstruct the following chronostratigraphy and provenance for the Las Chilcas Formation.

Unconformably overlying the Cerro Morado Formation, The Las Chilcas Formation can be subdivided into the four members described in section 3. The ages of each of these members have been estimated based on the new radiometric data and their stratigraphic relations that we detail below.

*Pitipeumo Member:* Estimated age range of ~105 to ~100 Ma. The provenance ages recorded in this member are identical to those inferred for the Cerro Morado Formation, confirming that the latter is the main source for the deposits of the lower to middle portion of the Pitipeumo Member. This is consistent with the  $112 \pm 1.3$  Ma U-Pb age obtained in the crystal-tuff clast (P16-2111) collected in the Pitipeumo Member.

A 30 m thick calcareous succession included by Thomas (1958) in the Las Chilcas Formation is exposed 20 km south of the study region and 35 km northwest of Santiago. These deposits, named Polpaico Limestones were thoroughly described by Gallego (1994) but have never been assigned to a precise stratigraphic position in the Las Chilcas Formation. We report a new U-Pb zircon age of  $103.2 \pm 0.7$  Ma obtained on an andesitic sample (PP3-1601) collected from a volcanic succession overlying the limestones near Punta Peuco (see locality in Figure 1). On this chronological basis, the Polpaico Limestones belongs to the base of Pitipeumo Member, thus a lateral equivalent of Unit B described in section 3.

*Tabón Member:* Estimated age range of ~100 to ~95 Ma. The provenance results obtained in the lower portion of the Tabón Member indicate that this member received debris solely from the volcanic levels of the Pitipeumo Member. Toward the middle to upper portion of this member, the main source recorded corresponds to a mixture of zircons from the coeval volcanic activity and from the underlying the Cerro Morado Formation. Scarce grains with ages of 160 and 173 Ma coincide with the age of the Jurassic batholith located in the present-day western slope of the Coastal Cordillera. However, according to Gana and Zentilli (2000), this batholith reached the surface only at circa 70 Ma. Therefore, these grains are either recycled or correspond to the Late Jurassic volcanic Horqueta Formation.

*Ñilhue Member:* Estimated age range of ~95 to ~91 Ma. In the only sample collected in this member, a single peak with an age similar to that of the top of the Cerro Morado Formation is likely due to a local paleogeographic condition. Where this sample was collected, in the Llanos de Portales area, the Pitipeumo Member is absent and the Tabón Member rests directly and unconformably on the Cerro Morado Formation, lacking direct sources of younger zircons. Hence, in this case the actual depositional age represented by the youngest zircon age is likely incorrect.

*El Calvario Member:* Estimated age range of ~91 to ~83 Ma. Some major differences show up when considering the provenance age of the detritic sample in this member in comparison with the underlying members. Well-defined peaks of 119 and 93 Ma come up in this member for the first time. The youngest one (93 Ma) coincides with the age of the youngest plutonic unit of the Caleu pluton (Molina, 2014). This is consistent with the exhumation age of the pluton determined by fission tracks data, which occurred between 94 and 90 Ma (Parada et al., 2005). The younger zircon grains of this peak (82 to 90 Ma) likely derive from the coeval volcanic activity evidenced by the frequent volcanic intercalations in this member. The older peak (119 Ma) coincides with the age of the Veta Negra Formation (Aguirre et al., 1999; Fuentes et al., 2005), in which the pluton was emplaced. Thus, despite its composition of andesites and basalts, this formation appears to be an important zircon source. This is consistent with the recurrent presence of andesite clasts containing large plagioclase phenocrysts (a typical characteristic of the Veta Negra Formation) in the El Calvario Member units. Three older and minor zircon peaks are also present in this Member; the first one (170 Ma) is similar to those scarce zircons present in the Tabón Member and hence are possibly recycled or correspond to zircons derived from the volcanic Horqueta Formation. The two oldest peaks of 289 and 303 Ma, although somewhat younger than the age of the Paleozoic Coastal Batholith (300 to 320 Ma from Deckart et al., 2014), might be recycled or originated from that batholith, which, according to the ages in Gana and Zentilli (2000), reached the surface at the same time that the El Calvario Member was deposited.

According to this new information, the Las Chilcas Formation would have an age range between 105 and 83 Ma. This age range coincides well with the ages assigned to other formations interpreted to be associated with the Peruvian tectonic phase by previous authors in Chile and elsewhere in the Andes, north and south of the study region.

### 6.2. Chronology of Deformation

Based on the sedimentologic, structural and chronologic evidence provided in this article it is possible to recognize that the transition period from the Early Cretaceous extension to the Late Cretaceous compressive phase spans from 116 to 105 Ma when the Cerro Morado Formation was deposited in a postrift tectonic setting (further described in sections 6.4 and 6.6). Subsequently, at least four periods of continuous compressive tectonism occurred from the Albian to the end of the Cretaceous.

The first tectonic period is coeval with the early stages of the Caleu Pluton emplacement and is evidenced by the erosion and angular unconformity exposed north of the Aconcagua Valley on the frontal limb of the Melón monocline between the Cerro Morado Formation and the Tabón Member. In this region, the younger Pitipeumo Member is absent, suggesting that uplift and erosion associated with this event either (i) eliminated the Pitipeumo Member or (ii) precluded its deposition. It may also be possible that there is an onlap relation between the Cerro Morado Formation and the Tabón Member, which could also involve the underlying Pitipeumo Member. In this case the Pitipeumo Member would wedge out before getting to the current surface. Nonetheless, the abrupt facies change from the Cerro Morado Formation to the Pitipeumo Member at 105 Ma and the clear folding and erosion process occurred to the Cerro Morado Formation before the Tabón Member was deposited indicate that the Pitipeumo Member represents the first orogenic deposits of the Las Chilcas basin.

The second compressive period occurs coevally with the emplacement of the last phase of the Caleu Pluton. This period is recorded by the unconformity between the Pitipeumo and Tabón members on the frontal limb of the Cerro Blanco anticline. Additionally, the deep incision in the Pitipeumo Member filled by the basal Tabón conglomerates and the growth strata geometry developed in these conglomerates to the east of the anticline's frontal limb, indicate that the anticline growth occurred, at least in part, simultaneously with the accumulation of the Tabón conglomerates. These thick molassic successions deposited in this subphase and the structures described above possibly define this as the stronger compressive period within this major compressive phase. The age obtained in the Tabón Member indicates that the deformation in this period occurred between ~100 and ~95 Ma.

The third deformation period is recorded by the Los Maquis backthrust, which developed after the deposition of the Tabón Member, being partially sealed by the El Calvario Member. Based on this, it can be concluded that the compressive period occurred coevally with deposition of the Ñilhue Member. An age of  $91.1 \pm 0.74$  Ma obtained at the base of the El Calvario Member, on top of the Los Maquis backthrust constrains the age of this deformation period. The absence of the Ñilhue Member in some sections south of the Aconcagua Valley might also reflect the deformation and erosion process generated during this period.

Finally, evidence for a fourth gentle deformation period is recorded by wide N-S folds in the El Calvario Member. This structure is unconformably covered by the almost flat-lying Lo Valle Formation, in which a sample close to its base yielded  $73.3 \pm 0.45$ , sealing and limiting the Late Cretaceous deformation phase.

These four compressive periods indicate the existence of a compressive regime throughout the Late Cretaceous and particularly all along the deposition of the Las Chilcas Formation. Its synorogenic nature occurred in relation to the development of compressive structures and growth strata. The thick molassic Tabón Member is regarded as the more remarkable orogenic record in this period (100–95 Ma).

### 6.3. Tectonic Implications Based on Provenance Results

Provenance analyses based on the detrital zircon ages described in section 6.1 reflect a pattern of depositional evolution for the Las Chilcas Formation that can be interpreted as the result of the exhumation of arc-related volcanic and intrusive units cropping out in the current Coastal Cordillera (Figure 8a).

Provenance variations document a normal unroofing of the mid-Cretaceous and Early Cretaceous arc sequences during this period. The units under erosion are recorded in this order: (1) erosion coeval volcanism of the Las Chilcas Formation, (2) erosion of the Cerro Morado Formation, and (3) erosion of the Veta

Negra Formation along with the Caleu Pluton. This sequence indicates that the bulk of the sediments supply into the Las Chilcas Formation came from these arc-related Cretaceous sources. At the same time a coeval exhumation of western older units as Jurassic sediments and Paleozoic intrusive units took place. This is recorded by apatite fission track exhumation ages of both Jurassic and Paleozoic intrusions in the Coastal Cordillera (Gana & Zentilli, 2000). However, only some rare Jurassic zircon grains are documented in the Las Chilcas Formation (in samples LC3-1509 and LV5-1709). This can be interpreted as a consequence of an exhumation process taking place in two structurally different uplifted blocks: the eastern block, which exhumated the arc-related Cretaceous volcanics, supplying sediments to the Las Chilcas Formation, and the western block uplifting and exhuming the Jurassic units, supplying sediments to the west and only locally to the Las Chilcas Basin.

The eastern block, which uplifted and exhumed the arc-related Cretaceous units, matches appropriately with the structural interpretation described below in section 6.4 for the inverted Cretaceous basins.

#### 6.4. Interpretation of the Deep Structure

The uplift, erosional and depositional evolution characterized above provides good approximation of the tectonic processes involved in the deposition of the Las Chilcas Formation. Still, representing the upper crust architecture by cross sections permits to interpret the overall vergency, deformation mechanisms and the controlling structures, which are key elements for the subsequent interpretation of the paleogeographic changes generated by the compressive periods described above. As indicated previously, little information could be obtained directly from observation of the fault planes, since there is practically no evidence to determine their geometry at depth. Thus, faults movements have been interpreted based on their effects on the exposed stratified succession and the contact with intrusive bodies. We present next two cross sections (Figure 8b), which are an interpretation of the structural model based on the inversion of previous normal faults in a half-graben array, that participated in the evolution of the extensional Early Cretaceous intra-arc basins. This west dipping half-graben array is preferred since it is consistent with the east vergence of the main structures throughout the area. In addition, this architecture has been consistently recorded in other Early Cretaceous basins in Chile as the Chañarcillo (Martínez et al., 2013) and the Quebrada Marquesa (Del Real & Arriagada, 2015) basins. Further justification for the interpretation of the deep architecture of every structure is described below; however, this model has not been tested in a restoration software; hence, different structural architectures may still be possible. The method how these sections were constructed is detailed in the supporting information section.

Although several N-S oriented normal faults have been mapped in the Veta Negra Formation in this and previous studies (Boric et al., 2002), no definitive structural evidence has been provided indicating extensional conditions during deposition of this volcanic unit. However, as previously described, the Veta Negra Formation is interpreted to have been deposited under extreme extensional tectonics on a thin continental crust (Vergara et al., 1995). The presence of roof pendants of the Veta Negra Formation (see cross section A-A' in Figure 8b) over the Caleu pluton, which was emplaced at 7 km depth (Parada et al., 2005), and the fact that some of the highest ridges (>2,000 m of altitude) of the Coastal Cordillera in this region consist of the Veta Negra Formation suggest that the structural style of the region can be related to inversion of a former extensional basins that accommodated the Early Cretaceous volcanics. Furthermore, similar features to those observed in the asymmetric, long-wavelength Cerro Blanco Anticline with a tight hinge and a steep frontal limb overlapped by growth strata have been reconstructed in analogue modeling experiments for the inversion of synrift sedimentary piles along a steep west dipping positively inverted listric fault (Gomes et al., 2006; McClay & Buchanan, 1992; Yamada & McClay, 2003).

Similar to what is observed in the Cerro Blanco anticline, but at a larger scale, the Melón monocline is an asymmetrical and long-wavelength fold with a steep east dipping frontal limb that reaches 45° east dip toward a NS lineament correlated with the Los Perros Fault. According with the previously described analogue models, the Melón monocline could also result from inversion of a deeply rooted west dipping inverted listric fault with a thick synrift volcano-sedimentary pile on the hanging wall, resulting in an inverted half-graben. This architecture would explain the extraordinary thickness of the Veta Negra Formation (up to 6,000 m), as the product of a deep-rooted master fault to the east and a thinning of the sequence to the west. The half-graben structure inversion during the Late Cretaceous is supported by the unconformity between the Cerro Morado Formation and the Las Chilcas Formation. The occurrence of several normal faults



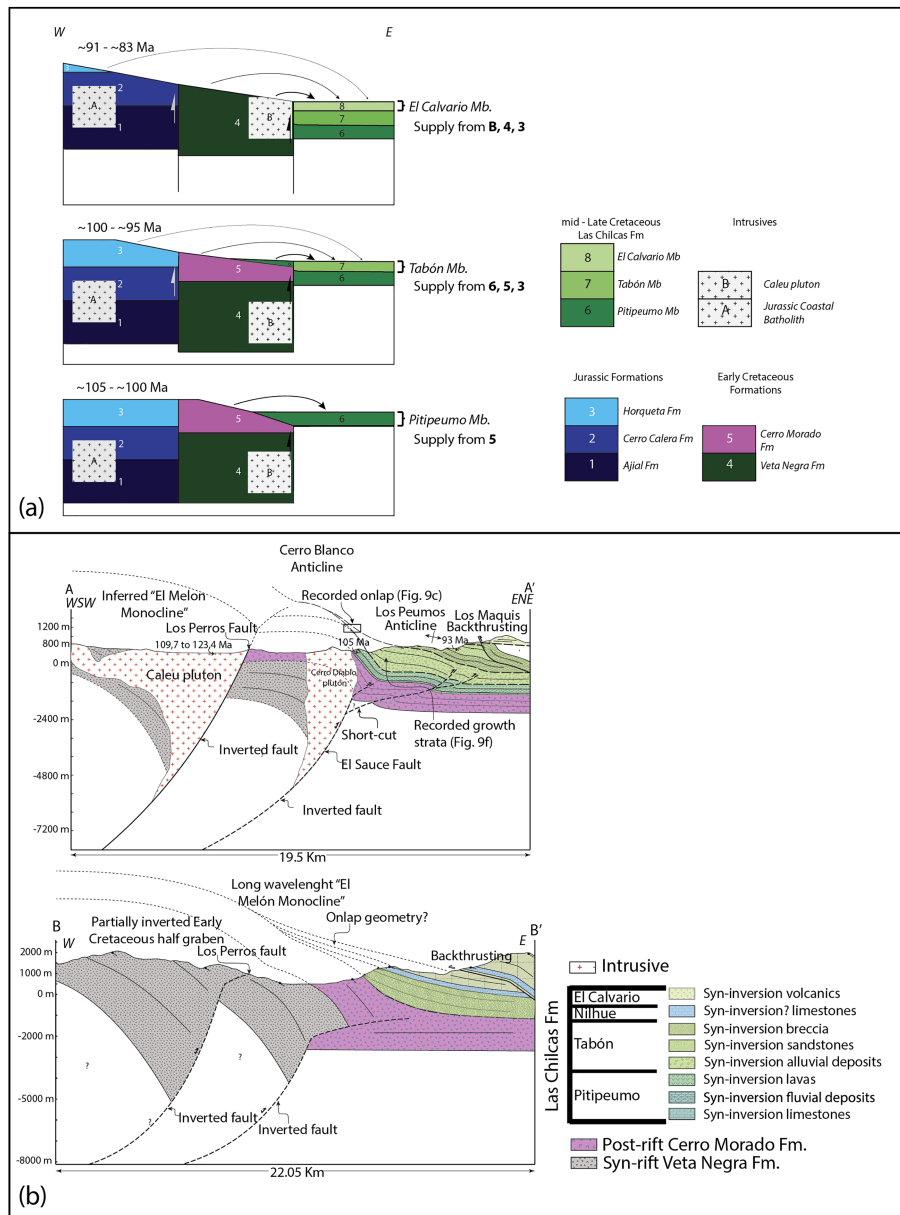


**Figure 8.** Structural and tectonic interpretations. (a) Sketch showing the interpreted provenance sources of the Pitipeumo, Tabón, and El Calvario members of the Las Chilcas Formation. (b) Cross sections; A-A' corresponds to south of the Aconcagua Valley and B-B' to the north of the same Valley (see explanation in the text).

affecting the Veta Negra Formation in the Melón monocline, with parallel strikes to the monocline, can be interpreted as accommodation antithetic and synthetic structures generated during the development of the monocline. To the south of the Aconcagua Valley, yet on the western side of the Los Perros Fault, the rapid exhumation of the Caleu Pluton between 97 and 93 Ma (Parada et al., 2005) also supports the existence of an important and deep-rooted structure uplifting the pluton. A hypothetical basal detachment deeper than 7 km would be needed to better reproduce the geometry of the Melón monocline. This deep detachment would also explain the 7 km exhumation of the Caleu pluton.

Inversion of a single thick-skinned normal fault, in this case the Los Perros fault, cannot reproduce some key structural features observed north and south of Aconcagua Valley such as the development of the Cerro Blanco anticline and its related thin-skinned deformation to the east and the 20–30° tilting of the Veta

Negra and Cerro Morado formations to the east of the Los Perros fault north of Aconcagua Valley. In consequence, another reverse or inverse fault with a ramp-flat geometry is necessary farther east (El Sauce Fault), conforming a couple of partially inverted half-grabens (“domino model”). In this model, the transition from the El Sauce fault ramp to an upper shortcut would allow: (i) the tilting of the Cerro Morado Formation and the overlying Las Chilcas Formation north of the Aconcagua Valley and (ii) the generation of the Cerro Blanco anticline, as represented in the cross sections.

According to this model the Veta Negra Formation has been deposited, at least in the eastern side of the intra-arc basin, in a half-graben structural array with listric faults controlling the deposition of the volcanic sequence. The Cerro Morado Formation represents the postrift deposits in which the El Sauce fault was propagated subhorizontally to the east, hindering the observation of the El Sauce fault in surface. Finally, the Las Chilcas sediments are deposited as the product of the inversion of the half-graben array.

### 6.5. Tectonic Setting of the Las Chilcas Basin

The tectonic phase that caused inversion of the described Early Cretaceous extensional basins created a major impact along the continental margin, including the development of the Las Chilcas basin. Integration of the different aspects related to the basin treated in this article suggests that the Las Chilcas Formation accumulated in a retro-arc position during mid-Cretaceous to Late Cretaceous contraction. The stratigraphic record and thickness of the accumulated sediments also suggest that during the initial stages of this period the floor of the basin reached the sea level and afterward was filled with synorogenic continental deposits and volcanic layers.

In foreland basin systems (DeCelles & Horton, 2003), the frontal part of the orogenic wedge is buried by syn-rotationally deformed wedge-top fluvial and alluvial sediments, characterized by immature and coarse textures and by growth structures and progressive unconformities. Frontal thrusts in this depozone are commonly blind, tipping out in the cores of fault propagation anticlines. These features indicate that wedge-top sediment accumulations are then deformed at or near the synorogenic erosional/depositional surface (as opposed to deeply buried deposits, isolated from the surface) (DeCelles & Giles, 1996).

In this context, the Las Chilcas Formation and particularly the Tabón Member compares well with the described lithofacies and structures from wedge top sediments. Also, consistent with this tectonic setting is the coeval arc proximity (the Caleu pluton emplaced directly the west of the basin deposits). The absence of postdepositional deformation and cannibalization of the Las Chilcas basin could be explained by the migration of the deformation front toward the foreland in the Late Cretaceous by a deep eastward propagating fault.

Deep-rooted structures controlled the evolution of the Las Chilcas basin on the eastern side of the uplifted arc; however, not much shortening has been accommodated at this time, despite the extended exhumation in the entire coastal range. Then, basin subsidence would be controlled by the high uplift rate and low shortening rate, which was not sustained at depth by crustal thickening. This can be regarded as a characteristic of the initial stages of this incipient foreland basin system. The described setting can also be assigned to the retroside basin of a subduction wedge as has been described by Comte et al. (2019).

### 6.6. Paleogeographic Evolution of the Las Chilcas Basin

It is described next a summary of the Cretaceous paleogeographic evolution based on the stratigraphic, sedimentologic, chronologic, and structural results obtained in this study (Figure 9).

Between 116 and 105 Ma, volcanic activity associated with tectonic extension ceased in the Veta Negra basin. Immediately after, arc activity resumed with a more explosive volcanism, covering the previous deposits and basin margins with 1,500 m of pyroclastic and lava material of the Cerro Morado Formation.

Basin inversion began at ~105 Ma; at this moment the Veta Negra basin was partially uplifted by the Los Perros fault. The considerable uplift generated subsidence to the east of the main structures, creating a retro-arc basin, which was initially filled with sea water. This setting is revealed by the existence of the marine limestones described in this study and by Arévalo (1992) at the bottom of the Pitipeumo Member. The basin was subsequently filled with fluvial, alluvial, and volcanic deposits represented in

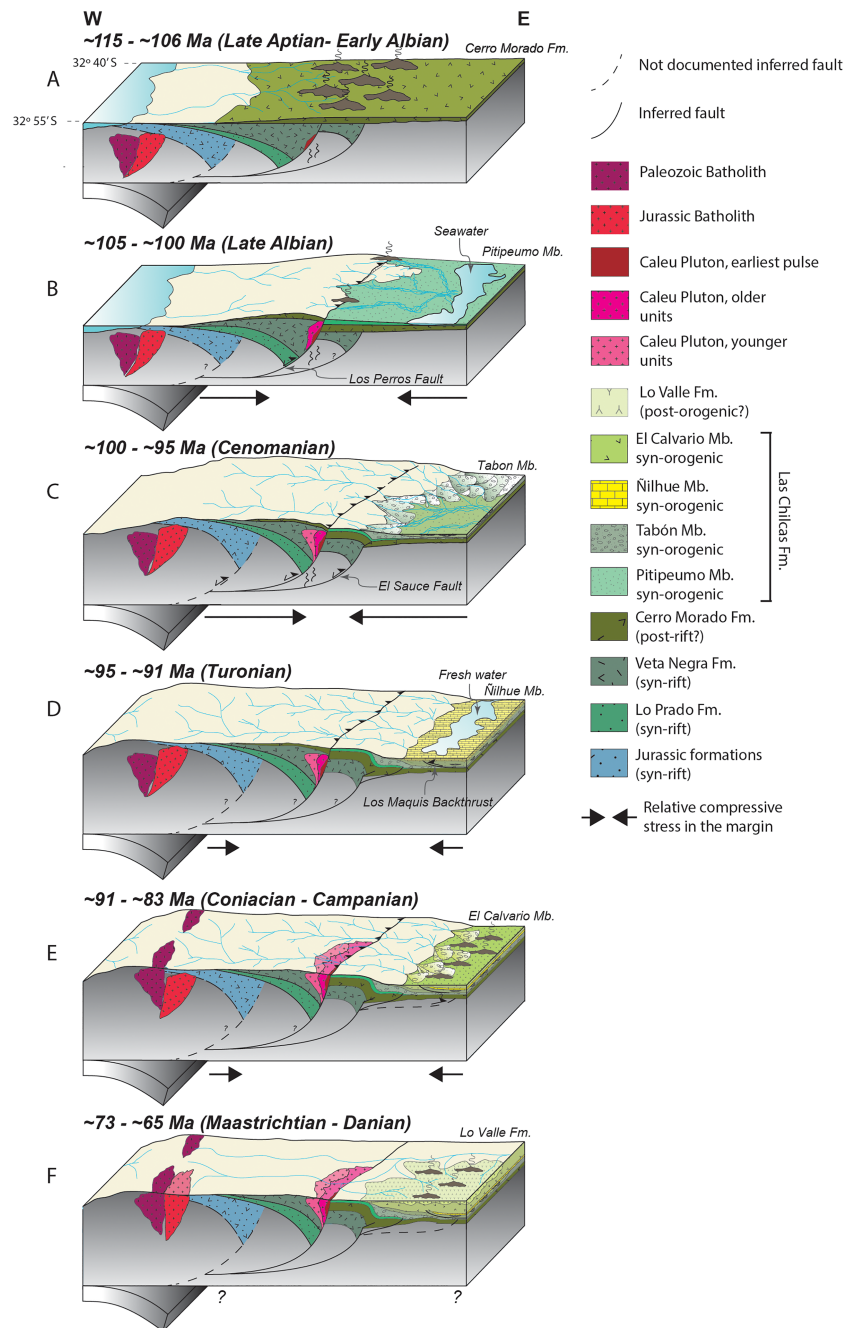


Figure 9. Paleogeographic and tectonostratigraphic evolution of the study area. Details in main text.

the middle and upper portions of the Pitipecmo deposits. This first compressive period is coeval with the exhumation event recorded in the intrusive rocks of the Coastal Cordillera between 106 and 98 Ma by Gana and Zentilli (2000).

During the Cenomanian (100–95 Ma) further deformation is recorded by the Cerro Blanco anticline growth. Its uplift caused an initial accumulation of coarse-grained alluvial fan succession on the foothills of the anticline. These deposits were subsequently covered by high-energy wandering fluvial deposits, represented by the upper portion of the Tabón Member. During this period inversion caused uplift of the westernmost blocks of the Andean margin permitting erosion of the Jurassic intra-arc successions. Probably, the high

compressive stresses caused cessation of the volcanic activity and the magmas remained captured in the continental crust forming the deep-seated Caleu pluton.

In the Turonian (95–91 Ma) the retro-arc basin was flooded again but this time by probably fresh water, creating conditions for deposition of the calcareous layers of the Ñilhue Member. In case that these limestones were marine (scenario discussed in section 3.3), the paths through which the ingression occurred are unknown. An explanation for the development of this short-lived marine or fresh water basin may be related to crustal bending caused by the load generated by the newly uplifted block. During this stage compression was still active and caused deformation on the more distal deposits, evidenced by the propagation of the Los Maquis backthrust. In the same period, between 94 and 90 Ma, the Caleu pluton experienced high exhumation rates (Parada et al., 2005), which strongly supports an important uplift phase and erosional activity in the eastern Coastal Cordillera at that time.

From 91 to 83 Ma, a thick succession of alluvial conglomerates and volcanic deposits represented by the El Calvario Member was deposited next to an important topographic relief along the arc. These deposits record the resumption of volcanic activity, but now on top of the proximal retro-arc basin deposits generated during previous stages, recording an eastward shift of the volcanic activity and possibly also the eastward migration of the basin axis. No direct evidence for compressional activity has been recorded during deposition of the El Calvario Member; however, the thick alluvial deposits in this member indicate a strong erosional activity centered in the reliefs west of the basin. A renewal of the compressive deformation is recorded toward the end of this stage by presence of a N-S oriented, gentle fold affecting the El Calvario Member below the unconformity that separates this member from the almost flat-laying tuffs of the Lo Valle Formation. The latter was deposited between 73 and 65 Ma, representing a renewal of intense arc volcanism and its definitive establishment farther east of the previous volcanic arc.

### **6.7. Tectonostratigraphic Relations With Other Middle to Late Cretaceous Deposits Along the Andean Margin**

Along the Andean continental margin there is vast evidence for a major tectonic phase representing a similar shift in tectonic and paleogeographic conditions to those described in this contribution, although the involved deposits do not always present the same characteristics.

In northern Chile, on the eastern flank of the Domeyko Range a mostly red-colored 4,000 m thick Cretaceous succession of continental detrital, mainly coarse deposits are represented by the Tonel, Purilactis and Barros Arana formations, included in the Purilactis Group (Bascañán et al., 2016; Mpodozis et al., 2005). Detailed sedimentological analyses and chronological ages on detrital zircons indicate a western and southwestern source for the deposits and have yielded ages of 107–83.6 Ma for the Tonel Formation and the lower Purilactis Group, and of 79–65 Ma for the upper Purilactis and Barros Arana formations. Based on the described features, the Purilactis Group has been interpreted in earlier studies in a similar way as has been the Las Chilcas Formation deposits, as the retro-arc foreland basin deposits located to the east of an uplifted relief formed during a major mid-Cretaceous compressive phase (Bascañán et al., 2016; Mpodozis et al., 2005). Farther north, similar deposits are grouped in the Cerro Empexa Formation in the western slope of the Altiplano. Even though its ages ranges are somewhat younger than the Las Chilcas Formation ages (85–65 Ma) (Morandé et al., 2015; Tomlinson et al., 2015), this unit also exhibits syncompressional deposition linked to basin inversion, with a synrift interruption during the Campanian (Morandé et al., 2015).

On the Principal Cordillera of Central Chile, in the Tinguiririca Valley, the Late Cretaceous Brownish-red Clastic Unit (BRCU) (Charrier et al., 1996; Tapia, 2015) is a 200 to 250 m thick sedimentary succession representing alluvial fan deposits at the base and alluvial plain deposits at its upper part. The BRCU unconformably overlies Late Jurassic marine deposits of the Baños del Flaco Formation, indicating that prior to deposition of the BRCU erosion removed the Early Cretaceous portion of the Baños del Flaco Formation and possibly also the overlying Colimapu Formation (Charrier, 1981; Charrier et al., 1996), removing an estimated thickness of ~2,000 m (Charrier, 1981). The general upward fining and thinning in the BRCU indicate retrograding deposition in a subsiding basin (Charrier et al., 1996). Recent datings on detrital zircon crystals in the BRCU confirm a Late Cretaceous age and provide maximum depositional ages between 96.4 and 83.8 Ma (Tapia, 2015), somewhat younger than the oldest ages than the Las Chilcas Formation. All this

evidence along with the existence of only Cretaceous components in the zircon populations of the BRCU (Muñoz et al., 2018; Tapia, 2015) suggests that it represents more distal deposits in the same Las Chilcas basin flanked to the west by the Cretaceous arc.

In the Mendoza-Neuquén basin of central southern Argentina, recent studies on two unconformably superposed mid-Cretaceous to Late Cretaceous sedimentary units—the Barremian to Aptian Bajada del Agrio and the Cenomanian to Campanian Neuquén Groups—provide important evidence for a major uplift and compressive deformation at this time (Di Giulio et al., 2017; Horton et al., 2016; Horton & Fuentes, 2016; Tunik et al., 2010). Recent studies deduced a major paleogeographic change at ~100 Ma based on (i) the unconformity between the mentioned units, (ii) a regional westward thickening of the Neuquén Group, (iii) syndepositional thrust faults, and (iv) major paleocurrents and detrital sources changes from one unit to the other. It was considered the cause of the change to be the uplift and exhumation of the Andean arc located to the west. Similarly, in the La Ramada basin in the northern portion of the Neuquén basin, a dramatic change in the detrital zircon provenance occurs from the lower section to the upper section of the Diamante Formation, between  $90.4 \pm 2.0$  and  $84.0 \pm 0.7$  Ma (Mackaman-Lofland et al., 2019). According to Mackaman-Lofland et al. (2019), this change initiates the supply of recycled zircons from Andean metamorphic complexes exhumed at that time. The arc exhumation would have resulted in the transition from a back-arc basin to a foreland basin setting in the Neuquén area. Complementing this idea, in the Malargüe area in the Argentinean foreland, Balgord and Carrapa (2016) suggested that initiation of the Malargüe thrust fold belt occurred at  $97 \pm 2$  Ma and that from this moment onward the Andean orogen was the main source for the deposits in the Neuquén basin.

The evidence from the Neuquén basin in Argentina indicate that deposition of the Diamante Formation and Neuquén Group units occurred in the middle and distal portions of the foreland basin, in the foredeep zone (Balgord & Carrapa, 2016; Horton et al., 2016; Horton & Fuentes, 2016), differently to the wedge-top setting interpreted for the Las Chilcas Formation. Besides, relevant chronologic differences can be identified between the Las Chilcas Formation and the Late Cretaceous Argentinean foreland deposits. For the latter, no tectonic change has been recorded prior to the 100 Ma erosional surface, differently to the first evidence for the onset of a compressive setting in the Las Chilcas Formation (105–100 Ma). This difference can be explained by the progression of deformation from west to the east; hence, the first structures were developed in the coastal region and then progressed eastward. Supporting this idea, Di Giulio et al. (2017) claimed that the regional scale uplift affecting the arc in Cretaceous time caused only slight tilt on the stratified levels in the external foreland because the initial uplift phase was caused by a large-scale continental folding during the initial stages of the compressive period (~100 Ma), before full development of thrust tectonics and retro-arc foreland basin development. This is consistent with the thick-skinned structures activity described for the Las Chilcas Formation in this contribution. The progression of the orogenic front toward the foreland during the Late Cretaceous has been well documented by Fennell et al. (2017) in the Malargüe thrust-fold belt. They claim that the orogenic front was 400–500 km east of the present-day trench in the late stages of the Late Cretaceous.

In the marine Rocas Verdes basin—southern Chile—a major coeval tectonic change is also reflected in the sedimentation conditions. A Late Jurassic extensional period was followed by subsidence and a marine incursion during Berriasian-Aptian time. In Aptian-Albian time, the area was affected by a tectonic phase that initiated the closure of the Rocas Verdes basin and subsequent development of a foreland fold-and-thrust belt, which resulted in exhumation and sediment supply to the foredeep (Cecioni, 1957; Malkowski et al., 2017). Although in a different environment, this evolution shows that a major and regionally extended tectonic phase occurred in mid-Cretaceous time in the central and southern Andes.

Other regions on the continental margin of South America show similar major modifications in mid-Cretaceous time (Horton, 2018a) supporting the regional existence and importance of this tectonic phase. These changes have been well documented in the Celica - Alamo basin in southern Ecuador (Jaillard et al., 1999), which extends southward to the Lancones basin, in northern Peru, and to the Querque basin, in southern Peru (Carlotto et al., 2009). In both basins, the Early Cretaceous deposits accumulated under extensional conditions. In the Lancones basin, a major change in the tectonic conditions is documented around 100 Ma and in the Querque basin in the Cenomanian. This major change in both basins is represented by an angular unconformity and has been interpreted to have been caused by inversion of the previous extensional basins.

## 7. Conclusions

1. A major tectonic and paleogeographic reorganization occurred along the western Gondwanan margin at the Early to Late Cretaceous transition. This phase originally named Peruvian Phase caused in Central Chile important arc uplift and exhumation.
2. The uplift of the arc and the exhumation of the associated intrusions are interpreted as caused by the inversion of Jurassic-Early Cretaceous basins.
3. As a consequence of this tectonic phase, a retro-arc basin, whose wedge-top deposits are recorded by the Las Chilcas Formation, was formed adjacent to the mid-Cretaceous to Late Cretaceous magmatic arc. This 3,000 m thick volcano-sedimentary succession represents the deposits resulting from the intense erosion affecting the uplifted Andean arc regions.
4. Provenance analysis in the Las Chilcas basin indicate a gradual uplift and unroofing of the Early Cretaceous volcanic arc from 105 to 85 Ma.
5. The Las Chilcas basin was dominated by high-energy synorogenic alluvial fan systems with volcanic influence. At the base of the Las Chilcas Formation, the record of a marine transgression suggest that the basin was initially close to the sea level and provide evidence of subsidence in the retro-arc.
6. The mid-Cretaceous to Late Cretaceous orogenic phase recorded in the Las Chilcas Formation is consistent with the arc exhumation and compressive evidence recorded in the Cretaceous foreland basins described at that time along the Andean margin.
7. The arc exhumation through deeply rooted reverse structures, the scarce shortening, and the disposition of a retro-arc basin inundated during its initial stages by marine water and afterward filled by continuous alluvial discharge with strong volcanic influence can be regarded as a characteristic response of a thinned crust to long-lived orogenic phases in subduction margins or, according to Comte et al. (2019) to the result of uplift and exhumation of a subduction wedge.

## Acknowledgments

This study was completed as a part of the senior author's MSc thesis. We acknowledge CONICYT, particularly for FONDECYT projects 1120272 and 1161806 to M. F., for funding this research. Daniel Boyce acknowledges the American Geophysical Union (AGU) for a travel grant to attend the AGU Fall Meeting 2014, where were presented the preliminary results of this study. The manuscript benefited from discussions with many researchers from the Geology Department of the University of Chile, particularly Luisa Pinto and Jacobus LeRoux, along with detailed reviews by Andrew Ryan and Daniel Müller from QPXC. The complete geochronological database is available in the following link (<https://figshare.com/s/dc2e72f3beba2daaa5a9>).

## References

- Aguirre, L., Féraud, G., Morata, D., Vergara, M., & Robinson, D. (1999). Time interval between volcanism and burial metamorphism and rate of basin subsidence in a Cretaceous Andean extensional setting. *Tectonophysics*, *313*(4), 433–447. [https://doi.org/10.1016/S0040-1951\(99\)00217-6](https://doi.org/10.1016/S0040-1951(99)00217-6)
- Arévalo, C. (1992). Facies ambientes de depositación y paleogeografía del miembro Pitipeumo (Formación Las Chilcas) V Región (BSc thesis). Universidad de Chile, Departamento de Geología.
- Balgord, E. A., & Carrapa, B. (2016). Basin evolution of Upper Cretaceous–Lower Cenozoic strata in the Malargüe fold-and-thrust belt: Northern Neuquén Basin, Argentina. *Basin Research*, *28*(2), 183–206. <https://doi.org/10.1111/bre.12106>
- Bascuñán, S., Arriagada, C., Le Roux, J., & Deckart, K. (2016). Unraveling the Peruvian Phase of the Central Andes: Stratigraphy, sedimentology and geochronology of the Salar de Atacama Basin (22 30–23 S), northern Chile. *Basin Research*, *28*(3), 365–392. <https://doi.org/10.1111/bre.12114>
- Blair, T. C., & McPherson, J. G. (1994). Alluvial fans and their natural distinction from rivers based on morphology, hydraulic processes, sedimentary processes, and facies assemblages. *Journal of Sedimentary Research*, *64*(3a), 450–489.
- Boric, R., Holmgren, C., Wilson, N. S. F., & Zentilli, M. (2002). The Geology of the El Soldado Manto Type Cu (Ag) Deposit, Central Chile. In T. M. Porter (Ed.), *Hydrothermal Iron Oxide Copper-Gold & Related Deposits: A Global Perspective* (Vol. 2, pp. 163–184). Adelaide: PGC Publishing.
- Boyce, D. (2015). Modelo de evolución tectónica y paleogeográfica del margen Andino en Chile central durante el Cretácico medio—Tardío: El registro estructural y sedimentario en la Formación Las Chilcas (MSc Thesis). Departamento de Geología, Universidad de Chile: 304p, Santiago, Chile.
- Carlotto, V., Quispe, J., Acosta, H., Rodríguez, R., Romero, D., Cerpa, L., et al. (2009). Dominios geotectónicos y metalogénesis del Perú. *Boletín de la Sociedad Geológica del Perú*, *103*, 1–89.
- Carter, W., & Aliste, N. (1962). Geology of the ore deposits of the Nilhue Quadrangle, Aconcagua province (unpublished report) Instituto de Investigaciones Geológicas, Chile.
- Cecioni, G. (1957). Cretaceous flysch and molasse in Departamento Última Esperanza, Magallanes, Chile. *American Association of Petroleum Geologists Bulletin*, *41*, 538–564.
- Charrier, R. (1981). Geologie der chilenischen Hauptkordillere zwischen 34°30' südlicher Breite und ihre tektonische, magmatische und paleogeographische Entwicklung. *Berliner Geowissenschaftliche Abhandlungen* (Doctoral dissertation), 36: 270 p., Berlin.
- Charrier, R., Pinto, L., Rodríguez, M. P., Moreno, T., & Gibbons, W. (2007). Tectonostratigraphic evolution of the Andean Orogen in Chile. In T. Moreno & W. Gibbons (Eds.), *The Geology of Chile* (pp. 21–114). Chile: The Geological Society.
- Charrier, R., Ramos, V. A., Tapia, F., & Sagripanti, L. (2015). Tectono-stratigraphic evolution of the Andean Orogen between 31 and 37° S (Chile and Western Argentina). *Geological Society, London, Special Publications*, *399*.
- Charrier, R., & Vicente, J. C. (1972). Liminary and geosyncline Andes: Major orogenic phases and synchronical evolutions of the central and Magellan sectors of the Argentine Chilean Andes. In *Solid Earth Problems Conference, Upper Mantle Project*, Buenos Aires, 1970, 2, 451–470.

- Charrier, R., Wyss, A., Flynn, J. J., Swisher, C. C. III, Norell, M. A., Zapatta, F., et al. (1996). New evidence for late Mesozoic-early Cenozoic evolution of the Chilean Andes in the upper Tinguiririca valley (35°S), central Chile. *Journal of South American Earth Sciences*, 9(5–6), 393–422.
- Comte, D., Farias, M., Roecker, S., & Russo, R. M. (2019). The Nature of the subduction wedge in an erosive margin: Insights from the analysis of aftershocks of the 2015 Mw 8.3 Illapel earthquake beneath the Chilean Coastal Range. *Earth and Planetary Science Letters*, 520, 50–62.
- Corvalán, J., & Vergara, M. (1980). Presencia de fósiles marinos en las calizas de Polpaico. Implicaciones paleoecológicas y paleogeográficas. *Revista Geológica de Chile*, p. 75–83.
- DeCelles, P., Gray, M., Ridgway, K., Cole, R., Srivastava, P., Pequera, N., & Pivnik, D. (1991). Kinematic history of a foreland uplift from Paleocene synorogenic conglomerate, Beartooth Range, Wyoming and Montana. *Geological Society of America Bulletin*, 103(11), 1458–1475. [https://doi.org/10.1130/0016-7606\(1991\)103<1458:KHOAFU>2.3.CO;2](https://doi.org/10.1130/0016-7606(1991)103<1458:KHOAFU>2.3.CO;2)
- DeCelles, P. G., & Giles, K. A. (1996). Foreland basin systems. *Basin Research*, 8(2), 105–123. <https://doi.org/10.1046/j.1365-2117.1996.01491.x>
- DeCelles, P. G., & Horton, B. K. (2003). Early to middle Tertiary foreland basin development and the history of Andean crustal shortening in Bolivia. *Geological Society of America Bulletin*, 115(1), 58–77.
- Deckart, K., Hervé, F., Fanning, C. M., Ramírez, V., Calderón, M., & Godoy, E. (2014). U-Pb Geochronology and Hf-O Isotopes of Zircons from the Pennsylvanian Coastal Batholith, South-Central Chile. *Andean Geology*, 41(1), 49–82.
- Del Real, I., & Arriagada, C. (2015). Inversión tectónica positiva en el distrito El Espino: Relaciones entre deformación, magmatismo y mineralización IOCG, Provincia de Choapa, Chile. In Sociedad Geológica de Chile, Congreso Geológico Chileno, XIV, La Serena, Chile.
- Di Giulio, A., Ronchi, A., Sanfilippo, A., Balgord, E. A., Carrapa, B., & Ramos, V. A. (2017). Cretaceous evolution of the Andean margin between 36° S and 40° S latitude through a multi-proxy provenance analysis of Neuquén Basin strata (Argentina). *Basin Research*, 29(3), 284–304.
- Elgueta, S., Hodgkin, A., Rodríguez, E., & Schneider, A. (1990). The Cerro Negro mine, Chile: Manto-type copper mineralization in a volcanoclastic environment. In *Stratabound ore deposits in the Andes* (pp. 463–471). Berlin, Heidelberg: Springer.
- Espinoza, W. (1969). Geología del distrito cuprífero de Cerro Negro; Provincia de Aconcagua (BSc thesis). Departamento de Geología, Universidad de Chile.
- Fennell, L., Folguera, A., Naipauer, M., Gianni, G., Rojas Vera, E., Bottesi, G., & Ramos, V. A. (2017). Cretaceous deformation of the southern Central Andes: Synorogenic growth strata in the Neuquén Group (35°30′–37°S). *Basin Research*, 29, 51–72.
- Fuentes, F., Feraud, B., Aguirre, L., & Morata, D. (2005). Ar-40/Ar-39 dating of volcanism and subsequent very low-grade metamorphism in a subsiding basin: Example of the Cretaceous lava series from central Chile. *Chemical Geology*, 214, 157–177.
- Gallego, A. (1994). Paleambiente y mecanismos de depositación de la secuencia sedimentaria que aflora en el sector de Polpaico, Región Metropolitana, Chile, (BSc thesis). Departamento de Geología, Universidad de Chile, 427 p.
- Gana, P., & Tosdal, R. M. (1996). Geocronología U-Pb y K-Ar en intrusivos del Paleozoico y Mesozoico de la Cordillera de la Costa, Región de Valparaíso, Chile. *Revista Geológica de Chile*, 23, 151–164.
- Gana, P., & Wall, R. (1997). Evidencias geocronológicas <sup>40</sup>Ar/<sup>39</sup>Ar y K-Ar de un hiatus Cretácico Superior-Eoceno en Chile Central (33°–33°30′ S). *Revista Geológica de Chile*, 24, 145–163.
- Gana, P., & Zentilli, M. (2000). Historia termal y exhumación de intrusivos de la Cordillera de la Costa de Chile central. In IX Congreso Geológico Chileno, Puerto Varas. Simposio Internacional sobre Magmatismo Andino, Actas (Vol. 2, pp. 664–668).
- Godoy, E. (1982). Geología del área de Montenegro, Cuesta de Chacabuco, Región Metropolitana: El “problema” de la Formación Lo Valle, 1. In III Congreso Geológico Chileno, Concepción, p. A124–A126.
- Godoy, E., Rayner, N., & Davis, B. (2006). Edad U-Pb Cretácica Temprana de ignimbritas y andesitas en la Depresión Central, VI Región, Chile: Implicancias geotectónicas. In XI Congreso Geológico Chileno, Antofagasta: Santiago, p. 229–232.
- Gomes, C. J., Martins-Neto, M. A., & Ribeiro, V. E. (2006). Positive inversion of extensional footwalls in the southern Serra do Espinhaço, Brazil—insights from sandbox laboratory experiments. *Anais da Academia Brasileira de Ciências*, 78(2), 331–344. <https://doi.org/10.1590/s0001-37652006000200012>
- Horton, B. K. (2018a). Tectonic regimes of the central and southern Andes: Responses to variations in plate coupling during subduction. *Tectonics*, 37, 402–429. <https://doi.org/10.1002/2017TC004624>
- Horton, B. K. (2018b). Sedimentary record of Andean mountain building. *Earth-Science Reviews*, 178, 279–309.
- Horton, B. K., & Fuentes, F. (2016). Sedimentary record of plate coupling and decoupling during growth of the Andes. *Geology*, 44(8), 647–650.
- Horton, B. K., Fuentes, F., Boll, A., Starck, D., Ramirez, S. G., & Stockli, D. F. (2016). Andean stratigraphic record of the transition from backarc extension to orogenic shortening: A case study from the northern Neuquén Basin, Argentina. *Journal of South American Earth Sciences*, 71, 17–40.
- Jaillard, E., Laubacher, G., Bengtson, P., Dhondt, A. V., & Bulot, L. G. (1999). Stratigraphy and evolution of the Cretaceous forearc Celica-Lancones basin of southwestern Ecuador. *Journal of South American Earth Sciences*, 12(1), 51–68.
- Keidel, J. (1925). Sobre la estructura tectónica de las capas petrolíferas en el oriente del territorio del Neuquén, Dirección General de Minas, Geología e Hidrología.
- Larson, R. L., & Pitman, W. C. (1972). World-wide correlation of Mesozoic magnetic anomalies, and its implications. *Geological Society of America Bulletin*, 83(12), 3645–3662.
- Mackaman-Lofland, C., Horton, B. K., Fuentes, F., Constenius, K. N., & Stockli, D. F. (2019). Mesozoic to Cenozoic retroarc basin evolution during changes in tectonic regime, southern Central Andes (31–33°S): Insights from zircon U-Pb geochronology. *Journal of South American Earth Sciences*, 89, 299–318. <https://doi.org/10.1016/j.jsames.2018.10.004>
- Malkowski, M. A., Schwartz, T. M., Sharman, G. R., Sickmann, Z. T., & Graham, S. A. (2017). Stratigraphic and provenance variations in the early evolution of the Magallanes-Austral foreland basin: Implications for the role of longitudinal versus transverse sediment dispersal during arc-continent collision. *Geological Society of America Bulletin*, 129, 349–371.
- Maloney, K. T., Clarke, G. L., Klepeis, K. A., & Quevedo, L. (2013). The Late Jurassic to present evolution of the Andean margin: Drivers and the geological record. *Tectonics*, 32, 1049–1065. <https://doi.org/10.1002/tect.20067>
- Martínez, F., Arriagada, C., Peña, M., Del Real, I., & Deckart, K. (2013). The structure of the Chañarcillo Basin: An example of tectonic inversion in the Atacama region, northern Chile. *Journal of South American Earth Sciences*, 42, 1–16.
- McClay, K., & Buchanan, P. (1992). Thrust faults in inverted extensional basins. In *Thrust tectonics* (pp. 93–104). Dordrecht: Springer.
- Mégard, F. (1984). The Andean orogenic period and its major structures in central and northern Peru. *Journal of the Geological Society of London*, 141, 893–900.

- Miall, A. D. (1996). *The Geology of Fluvial Deposits*. Berlin: Springer Verlag.
- Molina, P. (2014). Geocronología y condiciones de cristalización de circones del Plutón caleu: Evidencias de su prolongada evolución tardimigmática (MSc thesis), Universidad de Chile.
- Morandé, J., Gallardo, F., Muñoz, M., & Fariás, M. (2015). Carta Guaviña (Carta Geológica de Chile 1:100.000, Serie Geología Básica: n.177). Región de Tarapacá: SERNAGEOMIN.
- Mpodozis, C., Arriagada, C., Basso, M., Roperch, P., Cobbold, P., & Reich, M. (2005). Late Mesozoic to Paleogene stratigraphy of the Salar de Atacama Basin, Antofagasta, Northern Chile: implications for the tectonic evolution of the Central Andes. *Tectonophysics*, *399*, 125–154.
- Mpodozis, C., & Ramos, V. A. (1990). The Andes of Chile and Argentina. In E. E. Erickson, M. T. Cañas Pinochet, & J. A. Reinemund (Eds.) *Geology of the Andes and its relation to hydrocarbon and mineral resources. Circumpacific Council for Energy and Mineral Resources, Earth science series* (Vol. 11, pp. 59–90). Huston, TX.
- Muñoz, M., Tapia, F., Persico, M., Benoit, M., Charrier, R., Fariás, M., & Rojas, A. (2018). Extensional tectonics during Late Cretaceous evolution of the Southern Central Andes: Evidence from the Chilean Main Range at ~35°S. *Tectonophysics*, *744*, 93–117. <https://doi.org/10.1016/j.tecto.2018.06.009>
- Oliveros, V., Morata, D., Aguirre, L., Féraud, G., & Fornari, M. (2007). Jurassic to Early Cretaceous subduction-related magmatism in the Coastal Cordillera of northern Chile (18°30′–24°S): Geochemistry and petrogenesis. *Revista Geologica de Chile*, *34*(2), 209–232.
- Parada, M. A., Féraud, G., Fuentes, F., Aguirre, L., Morata, D., & Larrondo, P. (2005). Ages and cooling history of the Early Cretaceous Caleu pluton: Testimony of a switch from a rifted to a compressional continental margin in central Chile. *Journal of the Geological Society*, *162*, 273–287.
- Rivano, S., Sepúlveda, P., Boric, R., & Espineira, D. (1993). Hojas Quillota y Portillo (Carta Geológica de Chile, v. 73, 1: 250.000). SERNAGEOMIN.
- Rivano, S., Sepúlveda, P., Boric, R., Herve, M., & Puig, A. (1986). Antecedentes radiométricos para una edad cretácica inferior de la Formación Las Chilcas. *Andean Geology*, 27–32.
- Rossel, P., Oliveros, V., Ducea, M. N., Charrier, R., Scaillet, S., Retamal, L., & Figueroa, O. (2013). The Early Andean subduction system as an analogue to island arcs: Evidence from across-arc geochemical variations in northern Chile. *Lithos*, *179*, 211–230. <https://doi.org/10.1016/j.lithos.2013.08.014>
- Sánchez, M. (1968). Estudio geológico de los yacimientos de Mantos Portales (BSc thesis), p. 159. Departamento de Geología, Universidad de Chile. Santiago, Chile.
- Scheuber, E., Bogdanic, T., Jensen, A., & Reutter, K. J. (1994). Tectonic development of the north Chilean Andes in relation to plate convergence and magmatism since the Jurassic. In *Tectonics of the southern central Andes* (pp. 121–139). Berlin, Heidelberg: Springer.
- SERNAGEOMIN (2003). Mapa Geológico de Chile (versión digital 1.0, 2003). SERNAGEOMIN, Santiago.
- Somoza, R., & Zaffarana, C. B. (2008). Mid-Cretaceous polar standstill of South America, motion of the Atlantic hotspots and the birth of the Andean cordillera. *Earth and Planetary Science Letters*, *271*(1–4), 267–277.
- Steinmann, G., Stappenbeck, R., Sieberg, A. H., & Lissón, C. I. (1929). Geologie von Peru.
- Suppe, J., & Medwedeff, D. A. (1989). Geometry and kinematics of fault-propagation folding. *Helvetica*, *83*(3), 409–454.
- Tapia, F. (2015). Evolución tectónica y configuración actual de los Andes centrales del sur (34°45′–35°30′S) (Doctoral dissertation). Departamento de Geología, Universidad de Chile.
- Thomas, H. (1958). Geología de la Cordillera de la Costa entre el Valle de La Ligua y la Cuesta de Barriga (1:50.000). Instituto de Investigaciones Geológicas, Santiago, Chile.
- Tomlinson, A., Blanco, N., & Ladino, M. (2015). Carta Mamiña (Carta Geológica de Chile 1:100.000, Serie Geología Básica), Región de Tarapacá, SERNAGEOMIN.
- Tunik, M., Folguera, A., Naipauer, M., Pimentel, M., & Ramos, V. A. (2010). Early uplift and orogenic deformation in the Neuquen Basin: Constraints on the Andean uplift from U-Pb and Hf isotopic data of detrital zircons. *Tectonophysics*, *489*(1–4), 258–273. <https://doi.org/10.1016/j.tecto.2010.04.017>
- Tunik, M. A., & Álvarez, P. (2008). Análisis y edad de la sección calcárea de la Formación Las Chilcas (Chile) y sus implicancias para la correlación con unidades de Argentina. *Revista de la Asociación Geológica Argentina*, *63*(3), 363–379.
- Vergara, M., Levi, B., Nyström, J. O., & Cancino, A. (1995). Jurassic and Early Cretaceous island arc volcanism, extension, and subsidence in the Coast Range of central Chile. *Geological Society of America Bulletin*, *107*, 1427–1440.
- Viteri, E. (1970). Estudio geológico de la región de los Cerros Negros y Portales. Provincia de Aconcagua (BSc Thesis), Departamento de Geología, Universidad de Chile.
- Wall, R., Sellés, D., & Gana, P. (1999). Área Tiltill-Santiago (Carta Geológica de Chile 1:100.000, Serie Geología Básica, N. 11). Región Metropolitana: SERNAGEOMIN.
- Windhausen, A. (1931). Geología Argentina, Segunda parte. Geología histórica y regional del territorio argentino. Casa Jacobo Peuser Ltda, Buenos Aires.
- Yamada, Y., & McClay, K. (2003). Application of geometric models to inverted listric fault systems in sandbox experiments. Paper 1: 2D hanging wall deformation and section restoration. *Journal of Structural Geology*, *25*, 1551–1560.

## References From the Supporting Information

- Dickinson, W. R., Lawton, T. F., & Gehrels, G. E. (2009). Recycling detrital zircons: A case study from the Cretaceous Bisbee Group of southern Arizona. *Geology*, *37*(6), 503–506. <https://doi.org/10.1130/G25646A.1>
- Paton, C., Woodhead, J. D., Hellstrom, J. C., Hergt, J. M., Greig, A., & Maas, R. (2010). Improved laser ablation U-Pb zircon geochronology through robust downhole fractionation correction. *Geochemistry, Geophysics, Geosystems*, *11*, Q0AA06. <https://doi.org/10.1029/2009GC002618>
- Petrus, J. A., & Kamber, B. S. (2012). VisualAge: A novel approach to laser ablation ICP-MS U-Pb geochronology data reduction. *Geostandards and Geoanalytical Research*, *36*(3), 247–270.